DEVELOPMENT AND TESTING OF A MULTI-LAYER SOIL-ROLLER INTERACTION MODEL

A Dissertation

by

DANIEL JOSEPH RICH

Submitted to the Office of Graduate Studies of
Texas A&M University
in partial fulfillment of the requirements for the degree of

DOCTOR OF PHILOSOPHY

December 2010

Major Subject: Civil Engineering

DEVELOPMENT AND TESTING OF A MULTI-LAYER SOIL-ROLLER INTERACTION MODEL

A Dissertation

by

DANIEL JOSEPH RICH

Submitted to the Office of Graduate Studies of
Texas A&M University
in partial fulfillment of the requirements for the degree of

DOCTOR OF PHILOSOPHY

Approved by:

Chair of Committee, Robert L. Lytton
Committee Members, Charles Aubeny
Christopher C. Mathewson
J. Don Murff
Head of Department, John Niedzwecki

December 2010

Major Subject: Civil Engineering

ABSTRACT

Development and Testing of a Multi-layer Soil-roller Interaction Model.

(December 2010)

Daniel Joseph Rich, B.S.C.E., Rose-Hulman Institute of Technology;

M.C.E., The University of Houston

Chair of Advisory Committee: Dr. Robert L. Lytton

This dissertation focuses on the development of a mechanics based soil-roller interaction model intended to determine the degree of compaction of the top soil layer. The model was calibrated with, and compared to, soils data obtained from field and laboratory tests. The model contained 2 soil layers, but can be expanded to include additional layers.

This study concludes that the developed soil-roller interaction model is capable of accurately determining the degree of compaction of the upper soil layer through back calculation of the soil modulus values. The model was able to reach convergence between the calculated and measured values of roller drum deflection through a regression analysis of soil stiffness and damping characteristics. The final values of the stiffness and damping characteristics needed to achieve a 1% difference between the calculated and measured values of roller drum deflection fell within expected ranges for the type of material tested.

Part of this study included a sensitivity analysis of the input characteristics. The results of the sensitivity analysis revealed that the output of the model was highly sensitive to the mass of the second soil layer and to the elastic and plastic stiffness characteristics within both soil layers, but relatively insensitive to the mass of the first soil layer. The lack of sensitivity to the mass of the first soil layer means that large changes in the layer mass, and by extension the density, will have little effect on the output of the model. This characteristic is a drawback for conventional, density based

specifications. However, specifications based on installing fill to the designed values of stiffness or modulus could benefit from the model.

Much of the initial difference between calculated and measured roller drum deflection was probably caused by the difficulty in determining accurate starting values for the soil stiffness, damping and mass model characteristics. Future research should focus on ways to determine accurate values of the required input characteristics.

ACKNOWLEDGEMENTS

Thanks to the current and former members of my dissertation committee, Robert Lytton, Charles Aubeny, Chris Mathewson, Don Murff, and Tanner Blackburn, for their patience, guidance, and encouragement throughout this multi-year odyssey. A special thanks to Robert Lytton for believing that an older dog could learn new tricks and for encouraging me to pursue a Ph.D. when others said I should not. Thanks also to Tom Scullion for convincing me that I had the time to come and work for him on the Roller Acceleration Monitoring (RAM) system project, which provided the data used to test the accuracy of the soil-roller interaction model.

A number of people within the Texas Transportation Institute played key roles in the development and testing of the RAM system and deserve mention, Tony Barbosa, Stephen Sebesta, Wenting Liu, Lee Gustavous, Lupe Fattorini, Pat Harris, and Tom Scullion. Without their tireless work and dedication to the project, often in the middle of an active construction project during the blazing Texas summer, the needed data could not have been gathered. Thanks also to Stacy Hilbrich for helping to make TTI a fun place to work.

Rong Luo's extensive knowledge of MATLAB and Excel was indispensible in testing the model. If I had to learn MATLAB, or worse, take partial derivatives of a twenty term equation with respect of fourteen real and imaginary characteristics by hand, the model would never have been tested. To her I offer a most relieved thank you.

Thanks also to my colleague, Dr. Richard Tonda of SEA Limited for reviewing the step-by-step derivation of the soil-roller interaction model in spite of a hectic work and family schedule.

Funding for the RAM system project was provided by the Texas Department of Transportation. Without its willingness to fund research projects many new innovations, such as the RAM system, would never see the light of day. Thanks to German Claros, Roy Pilgrim, Darlene Goehl and Mike Arellano.

Lone Star Infrastructure and Young Brothers Construction allowed us access to several projects in order to test the RAM system under field conditions. Thanks to these two organizations for allowing us to get in their way in the name of science. Finally, to my parents and family, and to the teachers, formal and informal, that I have had throughout my life: thanks for sharing a part of yourselves with me.

TABLE OF CONTENTS

LIST OF FIGURES

LIST OF TABLES

CHAPTER I
INTRODUCTION

GENERAL

The current methodology of establishing and controlling compaction of pavement subgrade and base materials, and embankment fills, is based on achieving specified densities or unit weights within each layer of the placed material. The terms unit weight (weight per unit volume) and density (mass per unit volume) are often used interchangeably in the literature when discussing compaction. This convention can create a degree of confusion unless one bears in mind that under the U.S. system of measure scales are generally programmed to display weights (pounds and ounces), not mass (slugs). Scales reporting in metric units usually display mass (grams) rather than force (Newtons). Both systems of units were used during this research project. The values measured during the project are reported in the text with approximate conversions immediately following in parentheses.

Many government agencies base their quality assurance (QA) and acceptance programs on random, in-place unit weight measurements and/or laboratory analysis of core samples (Brock and Sutcliffe, 1986; McCarthy, 2007; Spangler and Handy, 1982; TxDOT, 2005). These methods generally test much less than 1% of the placed material (TxDOT, 2005; Thurner and Sandstrom, 2000). As such, a strong possibility exists that some areas will be over or under compacted and that the each layer will not have a uniform density or support profile (TxDOT, 2005). This lack of uniformity can result in uneven pavement settlement under traffic loads, which could accelerate surface distress (Haas et al., 1994).

This dissertation follows the style of Soil & Tillage Research.

Methods of testing the compaction of approximately 100% of each layer of compacted material have been in use in several European countries for a number of years and efforts have been made to introduce the technology into the U.S. marketplace (Anderegg and Kaufmann, 2004; Peterson et al., 2007; Thurner and Sandstrom, 2000). The majority of these methods are based on attaching 1 or more accelerometers to a vibratory smooth drum roller and correlating the measured displacement of the roller drum to soil stiffness or resistance to deflection. An onboard data processing and display system allows the roller operator to give more attention to under compacted areas while avoiding areas that have already been adequately compacted (Anderegg and Kaufmann, 2004; Peterson et al., 2007; Rinehart and Mooney, 2005; Thurner and Sandstrom, 2000).

Unfortunately, the basic research behind the commercially developed systems is generally considered proprietary, which makes it difficult to independently verify the results and establish specifications. This difficulty led the Texas Department of Transportation (TxDOT) to contract with the Texas Transportation Institute (TTI) to develop and test an after-market compaction monitoring system for potential use by TxDOT and the construction community (Scullion et al., 2006). A large amount of experimental data was collected over the course of the system's 3 year development and testing period. These data included roller drum deflections, in-place densities and water contents, falling weight deflectometer and portable falling weight deflectometer readings, resilient moduli, and Atterberg Limits. Attempts to correlate the measured roller drum deflections with the degree of compaction of the top layer of tested material were unsuccessful. This general lack of correlation has also been verified by other researchers (Anderegg and Kaufmann, 2004; Peterson et al., 2007; Rahman et al., 2007; Scullion et al., 2006; Thurner and Sandstrom, 2000).

For this reason, it was decided that a mechanics based soil-roller interaction model should be developed in an attempt to isolate the degree of compaction of the top layer of compacted material from the influence of the underlying layers.

OBJECTIVE

The primary objective of this laboratory and field research study was the development and testing of a mechanics based, 2 layer, soil-roller interaction model that would allow for an accurate determination of the degree of compaction of the top soil layer. The degree of compaction was inferred by the amount of deflection of the instrumented vibratory roller drum during operation over the test sections. This convention was used because the measured mass of the top and underlying soil layers were needed to test the model. The model would be considered accurate if the measured and calculated amounts of roller drum deflections agreed within approximately 1%. The 1% threshold was selected because current methods of compaction measuring are considered to be acceptable if the errors are in this range (Padlo et al., 2005).

SCOPE

Numerous field and laboratory tests were conducted during the development of the Roller Acceleration Monitoring (RAM) system. These tests resulted in a significant amount of experimental data. Many of the field tests were conducted on active TxDOT road construction projects and at Texas A&M University's Riverside Campus. The mix of active construction projects, experimental test sections, and completed road beds provided a good cross-section of the material variability that would likely be encountered during commercial use.

A detailed discussion of the experimental methods used to gather the test data will be provided in Chapter IV. However, a brief summary of a typical testing protocol is as follows. Once a test section, usually 10 feet (3.05 m) wide by 100 feet (30.48 m) long, was selected within a specific project or test area, a series of test points would be laid out at 10 feet (3.05 m) increments along the centerline of the test section. Each of the 11 test points were evaluated by the available test equipment that might include; in-place density and water content (nuclear gauge), resilient modulus (falling weight deflectometer and portable falling weight deflectometer), and layer thickness (dynamic cone penetrometer). Soil samples were taken on 1 occasion to allow for laboratory

testing of density, water content, resilient modulus, Atterberg Limits, and unconfined compressive strength. The instrumented, vibrating roller was driven across the centerline of the test section several times and the test points were reevaluated to determine what, if any, changes in measured properties had occurred. The vibrating roller was again driven across the centerline of the test section several times and the test points were reevaluated a final time.

ORGANIZATION OF DISSERTATION

This dissertation is organized into 8 chapters. Chapter I describes the project objective and scope. Chapter II provides a brief overview of the relevant literature pertaining to compaction and compaction monitoring reviewed for this dissertation. Chapter III gives background information about TTI's RAM system, while Chapter IV explains the experimental methodology used to gather the field and laboratory data. Chapter V presents a brief discussion of the unsuccessful attempts to correlate the test data to the compaction level of the top soil layer. Chapter VI discusses the need for and the derivation of a mechanics based soil-roller interaction model to allow for the degree of compaction of the top soil layer to be isolated from the influence of the underlying layers. Chapter VII presents the results of the model testing using data obtained during the development of the RAM system. The findings and conclusions of this study, as well as recommendations for future research, are contained in Chapter VIII. The appendix provides the details of the derivation of the mechanics based, 2 layer, soil-roller interaction model.

CHAPTER II
BACKGROUND

GENERAL

This chapter briefly defines compaction as it relates to roadway and embankment construction, outlines the common current practices used to measure compaction, and summarizes the pertinent compaction literature reviewed for this dissertation.

COMPACTION

For the purposes of this dissertation, compaction is defined as the densification or stiffening of in-situ and/or imported material through the addition of mechanical energy (Holtz and Kovacs, 1981; Spangler and Handy, 1982). The most common pieces of compaction equipment used in roadway and embankment construction are rollers (Brock and Sutcliffe, 1986; Holtz and Kovacs, 1981; McCarthy, 2007; Mitchell and Soga, 2005; Spangler and Handy, 1982). While other methods of compaction, such as blasting or dynamic impact exist, they are not pertinent to this research. Compaction differs from consolidation in that compaction is a relatively rapid, artificial process, while consolidation is a slower process resulting from the application of long-term, usually static, loads, such as fill. Additionally, compaction involves the reduction of air voids in a material by particle rearrangement, whereas consolidation occurs when water and/or water and air are forced out of the soil matrix (Bardet, 1997; Fredlund and Rahardjo, 1993; Holtz and Kovacs, 1981; McCarthy, 2007; Mitchell and Soga, 2005).

CURRENT PRACTICE

The usual methods of establishing a material's compacted density are based on the work conducted by R. R. Proctor in California in the late 1920's and early 1930's (Bardet, 1997; Das, 1999; Holtz and Kovacs, 1981; Spangler and Handy, 1982). Proctor found that if the amount of compaction energy for a specific soil was held constant, that the addition of water would increase the dry unit weight up to a certain point. After that

point, which is known as the optimum water content, the further addition of water would decrease the dry unit weight. For purposes of roadway and embankment construction, the dry unit weight at the optimum water content is generally assumed to be the maximum dry unit weight that can be achieved with the available compaction equipment (Holtz and Kovacs, 1981; Yoder and Witczak, 1975). The degree of compaction called for in project specifications is typically a percentage of the Proctor maximum dry unit weight. Additionally, the specified dry unit weight must be obtained within a range of water contents slightly above or below the optimum water content (Brock and Sutcliffe, 1986; Holtz and Kovacs, 1981; Yoder and Witczak, 1975).

Whether or not a pavement subgrade, base material or embankment fill has reached its required degree of compaction is often determined by measuring the material's in-place density and water content at random locations within each layer (Brock and Sutcliffe, 1986). The target density and water contents are generally determined by performing laboratory compaction tests on representative samples of each subgrade or fill material to determine how density varies with water content for a specified amount of compaction energy (ASTM, 2001). Typical results of a Standard Proctor test are shown in Figure 2-1. The data in Figure 2-1 is for illustration purposes only and does not correspond to soil at any of the test sites. The peak of the curve denotes the maximum dry unit weight (approximately 120 pounds per cubic foot in this example), which was obtained when the sample was compacted at a water content of about 9.5%.

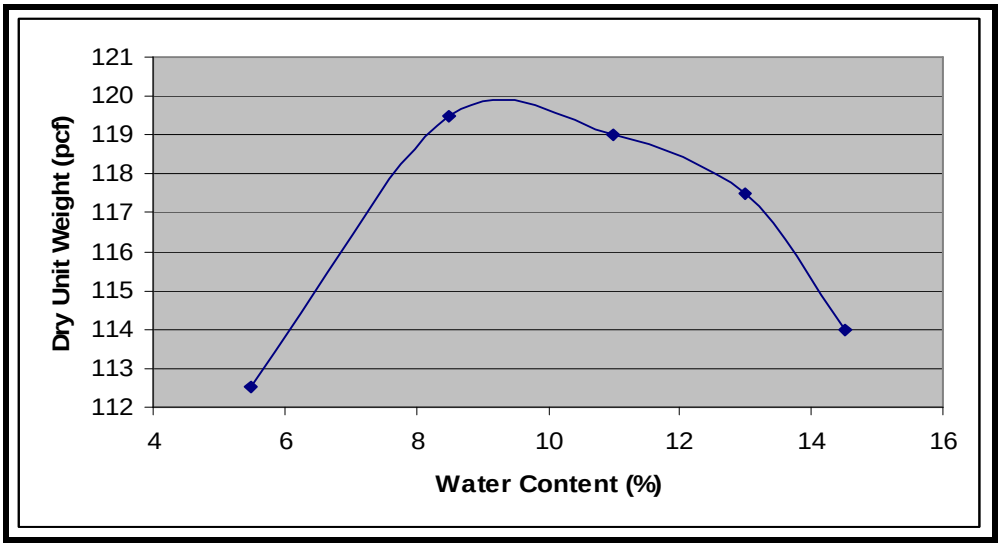

Fig. 2-1. Typical Proctor compaction curve.

There is some debate as to the exact role that the water added to a material on the dry side of optimum plays in compaction. One school of thought is that the water acts as a physical lubricant that allows the particles to move more easily past each other as they are aligned during compaction (Bardet, 1997; Das, 1999; Holtz and Kovacs, 1981). Another theory is that the dry soil has a high degree of suction that holds the particles tightly together and prevents their movement. The addition of water decreases suction and aids in compaction (Spangler and Handy, 1982). What is not generally debated is that there is a point where the addition of water, which is less dense than the soil particles, begins to take up space previously occupied by soil particles and thereby reduces the compacted material's dry unit weight (Bardet, 1997; Das, 1999; Holtz and Kovacs, 1981; Spangler and Handy, 1982).

A commonly used method of measuring the in-place density of compacted fill is the nuclear gauge. These gauges became widely used in the 1980's and provide a much quicker way of measuring density than the sand cone or liquid displacement methods (McCarthy, 2007). The gauges function by emitting gamma photons from a radioactive source into the material to be tested. In general, the more photons that are deflected

back to the detectors embedded within the gauge, the denser the material (Troxler, 2009). A drawback to the nuclear gauge is that its radioactive source necessitates careful storage, handling, and record keeping in order to abide by the numerous regulations governing the gauges (ASTM, 2001).

Pavements are not designed on the basis of the density of the various pavement layers; they are designed on the basis of each layer's modulus or strength (Haas et al., 1994; Huang, 2004; Yoder and Witczak, 1975). These values are assumed, incorrectly, to be uniform throughout each layer (Bardet, 1997; Das, 1999; Dunham, 1962; Fredlund and Rahardjo, 1993; Holtz and Kovacs, 1981; McCarthy, 2007; Mitchell and Soga, 2005; Spangler and Handy, 1982). Additionally, the random and minimalistic nature of some testing protocols can lead to a 10 to 40% chance that good material is rejected or that poor material is accepted (Spangler and Handy, 1982; TxDOT, 2005; Thurner and Sandstrom, 2000). To compound the problem, the inherently non-homogeneous nature of naturally occurring materials like soil almost guarantees that some areas of each layer will be over compacted while some areas will be under compacted (Thurner and Sandstrom, 2000).

Spangler and Handy (1982) found that over compaction can lead to the development of slickensides or shear-failure surfaces at the interface of the roller drum and the soil. These areas will be weak, even if the density specifications are met, and can lead to slope failures or other long-term performance issues. Under compacted materials can experience greater than expected settlements and may be weaker and more prone to erosion than soils that were compacted to the specified density (Das, 1999; Holtz and Kovacs, 1981; McCarthy, 2007; Spangler and Handy, 1982).

Methods of testing the compaction of approximately 100% of each compacted layer have been in use in several European countries for a number of years and efforts have been made to introduce the technology into the U.S. marketplace (Anderegg and Kaufmann, 2004; Thurner and Sandstrom, 2000). The majority of these methods are based on attaching 1 or more accelerometers to a vibratory roller and correlating the measured displacement of the roller drum to a material property such as stiffness. An

onboard data processing and display system allows the equipment operator to give more attention to under compacted areas while avoiding areas that have been adequately compacted (Anderegg and Kaufmann, 2004; Rinehart and Mooney, 2005; Thurner and Sandstrom, 2000; Scullion et al., 2006).

LITERATURE REVIEW

The study of compaction is not limited to civil engineering applications. The agronomy community has been interested in determining the level of compaction caused by the passage of farm equipment across fields for many years (Assouline, 2002; Ghezzehei and Or, 2001; Grift et al., 2005; Saeys et al., 2004). Engineers and agronomists are generally interested in finding the optimum level of compaction that will provide the most benefit to the project at hand, whether it be a roadway or a corn field (Assouline, 2002; Canillas, 2001; Jonsson et al., 2004; Or and Ghezzehei, 2002; Way et al., 2005).

Some of the pioneering work in vibratory compaction modeling was conducted by Tai-Sung Yoo and Ernest T. Selig (1979) in the late 1970's at the University of Massachusetts. Their research focused on, "the dynamic interaction of the soil-roller system, and the relationship of the system parameters to the amount of compaction." Their model consisted of: an idealized roller frame mass, a static drum mass with a rotating eccentric mass, and a single soil layer. The frame and drum and the drum and soil were separated by springs to model stiffness (resistance to deformation) and dashpots to model damping (resistance to motion). The results of their tests suggested that relationships existed between roller motions and the amount of compaction and that, "the key roller characteristic appears to be the magnitude of drum displacement during vibration."

Dieter Pietzsch and Wolfgang Poppy (1992) expanded upon the Yoo and Selig model in the early 1990's by separating the stiffness of the springs into elastic (recoverable deformation) and plastic (permanent deformation) components and by including a soil mass-spring-dashpot subsystem required to, "control the motion of the

soil mass during bounce operation of the drum (drum not in contact with the soil surface)." This model was primarily developed as a way to examine changes in compaction efficiency related to theoretical roller modifications rather than to determine the level of compaction of the upper soil layer. In fact, they stated, "Because of the complex effects inside of the soil it is not possible to describe the internal processes during compaction mathematically. Therefore, all model-based calculations can only approximate the actual vibration and compaction behavior."

Ghezzehei (2001) and Or (2002) have conducted work to determine the rheological properties of soils under varying stress conditions (steady state and oscillating) caused by climatic conditions such as wetting and drying of soil and mechanically applied loads. The determination of rheological properties allowed for the development of time-dependent stress-strain relationships that were used to develop models to predict changes in the level of compaction. Their findings indicated that soils with higher water contents behaved as viscoplastic materials under steady state loading, and as viscoelastic materials under loading caused by the passage of farm equipment (transient loading). Drier soils had a greater elastic component, or recovery of deformation, because of rapid, transient loading.

Methods of modeling or predicting soil compaction have also included correlation to the measured resistance of a cutting tool pulled through the soil at constant depth (Saeys et al., 2004) to methods involving monitoring the noise produced by a cone being pulled or pushed through the soil (Grift, 2005). Both methods were able to detect compacted zones or layers, but the disturbance of the compacted layer caused by drawing the instrument through the soil would render the layer unusable for roadway and embankment applications.

Heinz Thurner and Ake Sandstrom (2000) are well known in the field of continuous compaction control (CCC) or the constant monitoring of the compaction of a soil system. Their goal has been to develop a vibratory roller capable of providing a homogeneously compacted soil system by varying the amplitude and frequency of the eccentric, rotating mass that causes the roller drum to vibrate. Their results have

generally indicated that, “the result from a CCC - recording cannot - and should not – be expected to correspond to the density or to the compaction degree of the [top] layer – especially in fine grained materials at optimum or above optimum water content.” Or in other words, the response of the roller drum is a function of the entire soil system mobilized by the passage of the vibrating roller drum, not just the degree of compaction of the upper soil layer.

Anderegg and Kaufmann (2004) have also contributed to the CCC field. They have found that large amplitude, low frequency vibrations produce compaction at deeper depths than high frequency, low amplitude vibrations. They have also observed that as the level of compaction of a soil system increases there is a corresponding decrease in the level of damping. They have used these findings to develop a series of “intelligent” rollers that automatically adjust the frequency and amplitude of the roller drum vibration to produce homogeneously compacted soil systems.

The Minnesota Department of Transportation commissioned a study to evaluate a set of standard specifications for projects using intelligent compaction equipment (Peterson el al., 2006). According to the Peterson report, the standard specification required that, “a project- or site-specific intelligent compaction target value (IC-TV) is developed from a contractor-constructed control strip, using an approved IC roller, which measures or estimates in-situ stiffness or modulus, or another compaction related index parameter.” The study concluded that geostatistical methods were required to correlate the IC-TV to the degree of compaction of the tested material.

Intelligent compaction research performed by Kansas State University was similar to TTI’s approach in evaluating the degree of compaction of a specific lift (Rahman et al., 2007). The main difference between TTI’s study methodology, which is detailed in Chapter III, and the Kansas State University study was that TTI used an in-house manufactured monitoring system whereas Kansas State used commercially available intelligent compaction rollers. The Kansas State study concluded that the IC roller stiffness was sensitive to the water content of the compacted material and that no

single correlation existed between the IC roller stiffness and the results of traditional testing methods such as back calculated modulus.

Robert Rinehart and Michael Mooney (2005) of the Colorado School of Mines instrumented a double drum vibratory roller with 6 accelerometers (3 per drum) to monitor the roller's vibration characteristics during operation. The study was reportedly an intermediate step along the way to developing a model to determine the degree of compaction of subgrade and fill material. The testing and verification protocol for the roller was not detailed in the paper, but several conclusions were made. Among the conclusions was that changes in the level of compaction were reflected in changes in the phase lag angle and vibration characteristics of the roller.

SUMMARY

Attempts to model compaction have been on going for over 40 years. As discussed above, many of the modeling methods relied heavily on correlating measured parameters such as roller drum deflection to soil stiffness or a modulus. Correlation does not imply causation. In other words: just because a statistically significant line or curve can be drawn through a set of data points does not mean that the relationship will work in other circumstances. Some research undertaken within the last few years has attempted to use a mechanics based approach to develop a more portable mathematical model that can be calibrated to specific sites. The model discussed throughout the remainder of this dissertation is such a model.

CHAPTER III
ROLLER ACCELERATION MONITORING (RAM) SYSTEM

GENERAL

This chapter describes the RAM system developed by TTI for TxDOT. The system's composition and function are discussed and typical system outputs are shown. Additionally, the status of the system, which was transferred to TxDOT in 2008, is briefly discussed.

RAM SYSTEM COMPOSITION AND FUNCTION

TTI developed the prototype 100% coverage quality assurance system for TxDOT shown in Figure 3-1. The system measured the acceleration of a vibrating roller drum as the roller traveled across the layer surface. The prototype system was tested a number of times on varying sites to include active construction projects, manufactured test strips and gravel surfaced roads and parking lots. A great deal of roller drum acceleration and soil data was collected.

Accelerometer

The RAM system consisted of an accelerometer, which was mounted to a non-rotating portion of the roller drum assembly (Figure 3-2). The accelerometer was positioned between the vibrating drum and the isolation mounts so that only the acceleration of the drum was measured. The accelerometer contained a piezo-electric element that generated a current proportional to the amount of force that the element experienced by drum acceleration.

Fig. 3-1. Prototype roller system on SH 21 near Caldwell, Texas. Photograph courtesy of Dr. Wenting Liu.

Fig. 3-2. Accelerometer mounted on roller.

Prior to field testing, the accelerometer and the associated data acquisition system were calibrated in the laboratory. An exciter of known frequency and amplitude

was used to verify that the accelerometer was performing within specifications. The signal from the accelerometer passed through a signal conditioner that amplified and double integrated the signal to provide sensor displacement. This displacement was assumed to be essentially equal to the displacement of the roller drum because of the lack of damping between the roller drum and the accelerometer.

In the early field tests, the signal conditioner was housed in a padded box attached to the side of the roller as shown in Figure 3-3. The system provided to TxDOT had the signal conditioner, data acquisition system, and power supply housed in a box that was mounted in the roller operator's compartment to provide greater protection.

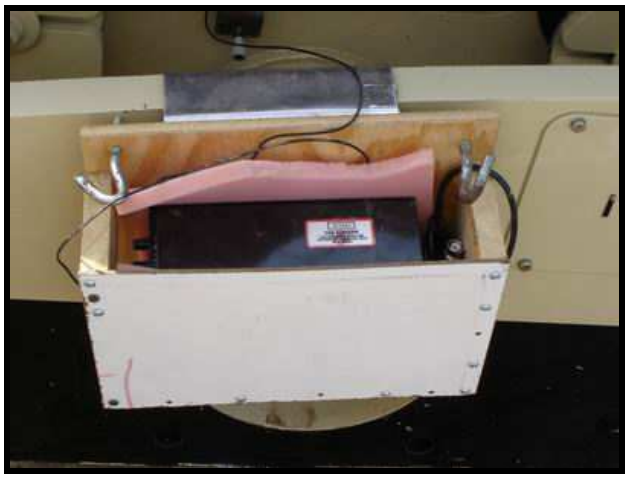

Fig. 3-3. Signal conditioner.

Distance Measuring Instrument

The position of the roller along the length of each test path was tracked by a distance measuring instrument (DMI) attached to 1 of the roller drive wheel hubs, as shown in Figure 3-4. The DMI functioned by counting the number of pulses caused by the inner mechanism rotating as the roller traveled down the test strip. Calibration of the DMI was required for each model of roller used and was accomplished by driving the

roller along a known distance and inputting the pulse count into the data acquisition and analysis software.

Fig. 3-4. Distance measuring instrument.

Data Acquisition System

The data acquisition system consisted of a rugged laptop computer, a National Instruments A/D card, and custom written software to collect, process, and display the measured data. The roller drum displacement and distance location information was typically sampled approximately 1,000 times per second. The raw roller displacement data from 1 of the runs of the system is shown in the upper plot of Figure 3-5. This is a plot of vertical drum movement versus horizontal distance along the test strip. This signal consisted of 2 superimposed waveforms. Low frequency displacements, between 0 and 3 Hertz (Hz), are caused by the movement of the roller over the ground and were an indication of surface roughness. High frequency drum displacements (32 Hz) are superimposed on these low-frequency displacements and are shown in the lower plot of Figure 3-5. It is these high-frequency displacements that are an indication of the degree

of compaction of the soil beneath the roller (Anderegg and Kaufmann, 2004; Thurner and Sandstrom, 2000; Yoo and Selig, 1979).

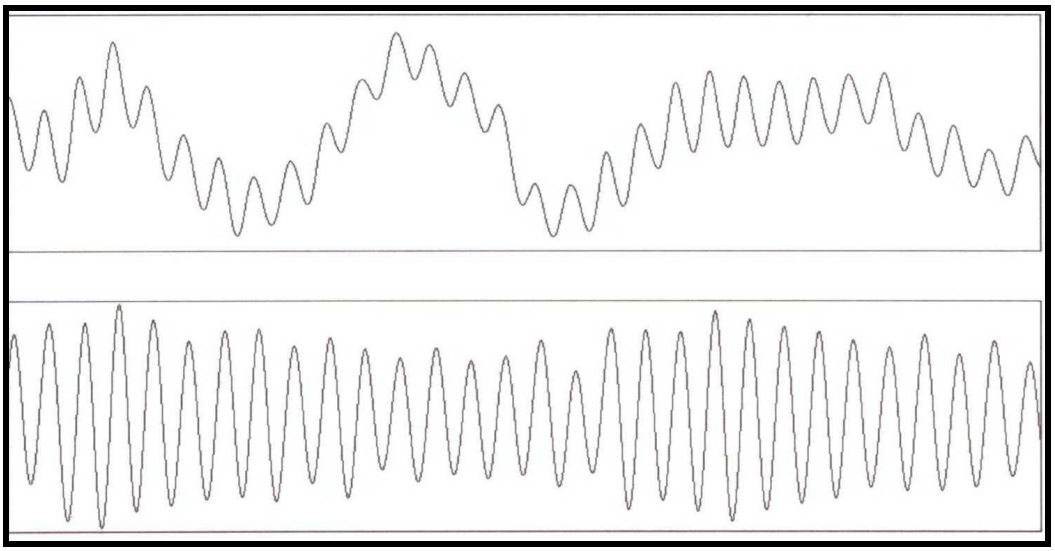

Fig. 3-5. Typical raw (top) and filtered (bottom) system output. Figure courtesy of Dr. Wenting Liu.

To decompose these signals, the raw data was processed through a Fast Fourier Transform which transformed the time domain into the frequency domain and allowed a frequency distribution plot to be produced. A frequency distribution plot shows the magnitude of the roller drum displacements on the Y axis in relation to the frequency at which the displacements occur along the X-axis. To separate the 2 components, a low pass band filter was applied to the data. Once filtering was completed a plot of roller displacement with distance was developed, as shown in the lower plot of Figure 3-5. Once the low frequencies associated with ground roughness were removed, the motion of the roller drum was measured by the system software. A typical frequency distribution plot is shown in the Appendix.

The deflection pattern shown in the lower plot of Figure 3-5 is judged as ideal. The peak to peak amplitudes show the displacement of the roller drum in contact with

the soil being compacted. However, on very stiff materials such as stabilized base courses or very dry, stiff clay a different deflection pattern was observed (Figure 3-6). The upper plot of the figure is the raw data, and the lower plot shows the motion of the drum. The lower plot shows a non-consistent set of amplitudes. This pattern was associated with cases where the roller drum was not in contact with the layer surface on every cycle of vibration (i.e. the roller was “double jumping”).

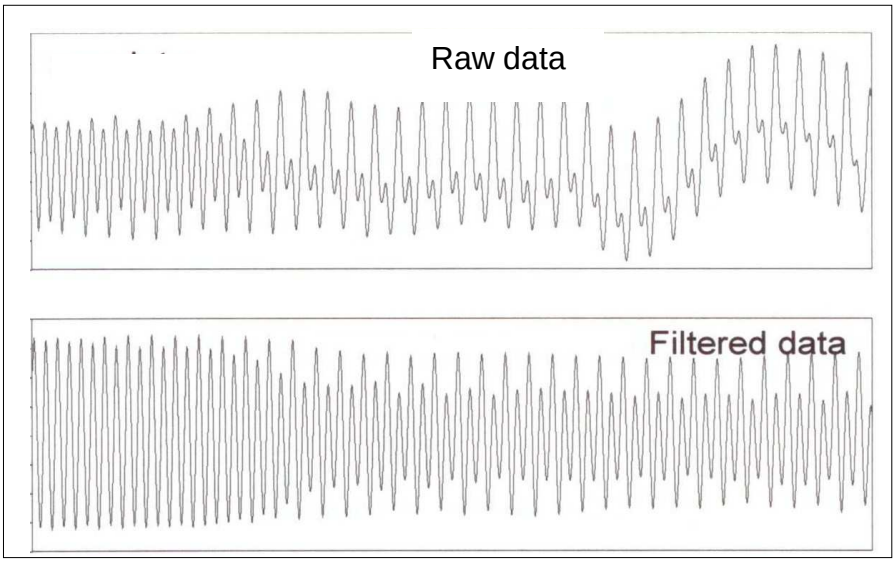

Fig. 3-6. Drum displacement during double jumping. Figure courtesy of Dr. Wenting Liu.

The final step in the data acquisition system was to measure the average peak-to-peak amplitudes and display those amplitudes against their location within the test strip. Analysis of the displacement versus location display allowed for areas with higher than average and lower than average displacements to be found. A typical roller displacement versus distance plot is contained in the Appendix.

RAM SYSTEM STATUS

Three RAM systems were delivered to TxDOT in 2008 for further field testing and evaluation. Difficulties with the software and the fragile nature of the electronic equipment have limited the usefulness of the system. The goal during the development of the system was to develop a correlation between roller drum displacement and the degree of compaction of the top soil/base layer.

Attempts to correlate drum deflection to a characteristic or property of the top soil/base layer such as strength, density, stiffness, or modulus have been unsuccessful, both by TTI and other researchers (Peterson et al., 2007; Rahman et al., 2007; Thurner and Sandstrom, 2006). Results of field tests of the prototype roller system indicated that the response of the roller is governed by more than just the upper few inches of the soil mass. This finding corresponds to the results reported by others in the literature (Peterson et al., 2007; Rahman et al., 2007; Thurner and Sandstrom, 2006). In order for a roller mounted system to be useful to government agencies and the construction industry, the system must be able to distinguish the effect of the top layer, which is being compacted, from the underlying layers, which have either already been accepted, or are not the responsibility of the contractor.

CHAPTER IV
EXPERIMENTAL METHODOLOGY

GENERAL

The RAM system was tested on a variety of soil and base course materials at Texas A&M University's Riverside Campus and on three active road construction projects in Texas (State Highway 6, State Highway 21 and State Highway 130). Some of the field testing was preformed with the sole intention of debugging the software and making the system easier to install and operate. As such, whatever data that was collected from those tests, which were primarily conducted at the Riverside Campus, was not rigorously analyzed for inclusion within the model. For the tests that were meant to gather roller and soil data, test strips ranging in length from approximately 100 feet (30.48 m) to over 1,000 feet (304.8 m) were laid out within each project. The following sections discuss the field and laboratory test protocols and equipment used during the evaluation program.

FIELD TESTING PROTOCOL AND EQUIPMENT

For test strips 100 feet (30.48 m) in length the following procedure was used. The initial material characteristics along the center line of each test strip were obtained at intervals of 10 feet (3.05 m) with several standard pieces of soil testing equipment prior to running the roller across the test strip. The equipment included; the nuclear density/moisture gauge, falling weight deflectometer (FWD), portable falling weight deflectometer (pFWD), and dynamic cone penetrometer (DCP). Not every piece of equipment was used on every project because of equipment non-availability and time constraints. Once the initial conditions at the prescribed points were established, the vibrating roller made 2 to 4 longitudinal passes along the centerline of the test strip and the standard equipment tests were again conducted at the prescribed points. An additional 2 to 4 longitudinal passes were then made along the test strip and a final set of standard equipment tests was conducted at the prescribed points.

For test strips longer than 100 feet, the vibrating roller was run along the center line of the strips. The output data was then analyzed in the field to locate areas with high and low roller deflections and areas with deflections approximately midway between the high and low deflections. Points meeting these criteria were tested with the available standard instruments to determine the in-place material characteristics.

A brief description of the standard test equipment is provided in the following sections.

Nuclear Density/Moisture Gauge

The nuclear gauge, shown in Figure 4-1, measures the wet and dry density and water content of the soil/base material from the surface down to approximately 12 inches (0.305 m) below the surface by means of a radioactive source. The radioactive source emits gamma photons which are reflected back to detectors within the instrument. In general, the greater the number of photons deflected back to the detectors the greater the density of the tested material (Troxler, 2009).

Fig. 4-1. Nuclear gauge. Photograph courtesy of Dr. Wenting Liu.

Falling Weight Deflectometer (FWD)

The falling weight deflectometer (Figure 4-2), functions by dropping prescribed weights from standard heights in order to simulate the passing of transient wheel loads. Seven geophones measure surface deflection at the center of the loading point and at 12 inch (0.305 m) intervals from the loading plate. The resulting set of deflections, which generally decrease with distance from the loading plate, is known as a deflection bowl. By knowing the shape of the deflection bowl, general material properties, and the approximate layer thicknesses, a resilient modulus for several layers can be back calculated using software programs such as MODULUS 6.0 (Lytton, 1989; Scullion et al., 1989).

Fig. 4-2. TxDOT falling weight deflectometer.

Portable Falling Weight Deflectometer (pFWD)

The pFWD, shown in Figure 4-3, is a much smaller version of the FWD. This unit measures vertical displacement of the surface at 3 points spaced 30 cm (11.81

inches) apart in response to a vertical impact load. A back calculated modulus is also determined by use of a supplied computer program.

Fig. 4-3. Portable falling weight deflectometer. Photograph courtesy of Dr. Wenting Liu.

Dynamic Cone Penetrometer (DCP)

The dynamic cone penetrometer (Figure 4-4) measures a material's resistance to penetration. The penetration energy is provided by raising a cylindrical hammer of constant mass to a constant height and then letting the mass freefall along a guide rod until the mass contacts the driving rod (Kessler, 2005). Analysis of the data defines layers within the test depth, normally up to 30 inches (0.762 m), by revealing changes in the slope of the penetration rate.

Fig. 4-4. Dynamic cone penetrometer. Photograph courtesy of Dr. Wenting Liu.

A typical DCP cumulative penetration versus depth graph is shown in Figure 4-5. The red arrow denotes the approximate depth at which the penetration rate changed from approximately 1 inch per blow to about 1/4 inch per blow. The change in penetration rate was caused by a change in 1 or more of the soil characteristics such as density, water content and/or shear strength. The change in penetration rate was assumed to denote the beginning of a new soil layer.

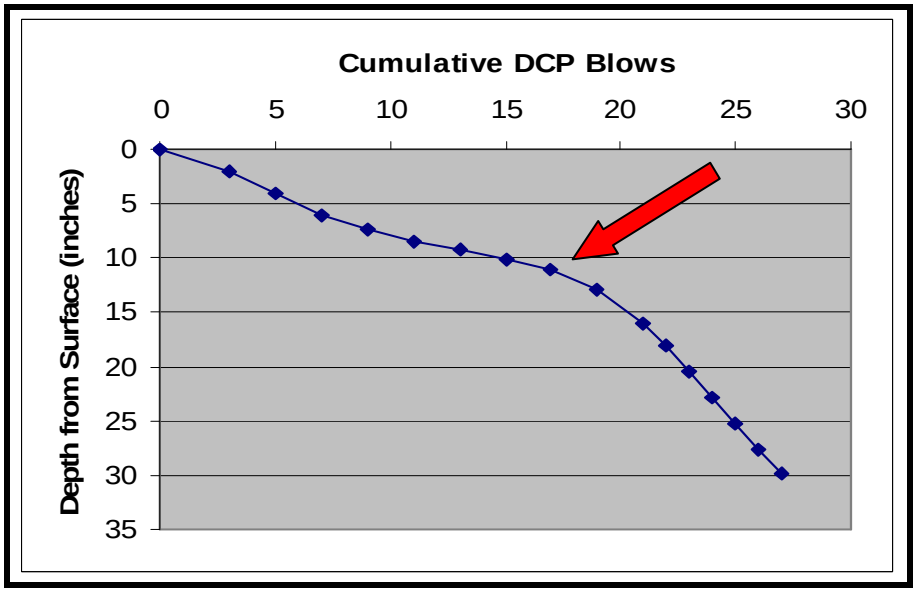

Fig. 4-5. Typical DCP penetration rate graph.

LAB TESTING PROTOCOL

Shelby tube soil samples were gathered by an outside geotechnical consulting firm on 2 of the SH 21 test strips after rolling was completed so that a series of laboratory tests could be conducted. The locations of the samples were determined by TTI and were selected in order to obtain soils data from locations with high, low and average measured roller drum accelerations. Four 2.8 inch (71.12 mm) diameter samples were taken to a depth of approximately 4 feet (1.22 m) at 6 different locations within the 2 test strips (total of 24 samples) and delivered to TTI for testing. The samples, which had been wrapped in foil and placed in plastic bags in the field, were stored in insulated coolers in TTI's humidity room in order to minimize moisture change prior to testing.

The laboratory tests included; wet and dry unit weight, water content, liquid and plastic limits, resilient modulus, and unconfined compressive strength. A brief description of each test and why the test was conducted, is provided below. It should be noted that while continuous sampling was conducted by the drilling crew, continuous

recovery was not possible. As such, it is possible that some of the tested samples contained material from multiple layers, which could skew the results.

Wet and Dry Unit Weights

Specifications for road and embankment fill usually require that the material must be compacted to a percentage of the material's maximum dry unit weight as outlined in the Current Practice section of Chapter II. For this reason, TTI made every effort to take unit weight readings during our testing protocol. The laboratory determination of unit weights was done to verify the results obtained with the Troxler nuclear gauge and to determine the unit weights of samples deeper than the effective test depth of the nuclear gauge, which is approximately 12 inches (30.48 cm) (Troxler, 2009).

The wet and dry unit weights were calculated using cylindrical samples that had been trimmed for the resilient modulus tests. The height and circumference of each sample was measured in three places, and the average value of each dimension was used to calculate the volume of each sample. The water content of the sample was found by taking the average of the water content of 3 samples of the soil trimmings removed from the top and the bottom of the each sample.

Water Content

The water content of a sample is a comparison of the weight of the water in a sample compared to the weight of the solids within the sample. The result is usually expressed as a percentage. It is possible for soil to have water contents greater than 100%.

Water content tests were conducted in general accordance with the appropriate ASTM procedure.

Liquid and Plastic Limits

The liquid limit and the plastic limit are two of the Atterberg Limits developed in the early 1900's by Swedish soil scientist A. Atterberg (Holtz and Kovacs, 1981). The Atterberg Limits are water contents that represent standardized demarcations between states of cohesive soil consistency. The states of soil consistency are defined as; liquid, plastic, semisolid and solid (Liu and Evett, 2008). For example, the liquid limit is the water content at which a soil has reached the lower limit of viscous flow or transitions between the liquid and plastic states (Holtz and Kovacs, 1981; Liu and Evett, 2008). This is not to say that soils with water contents above the liquid limit flow like water. It simply means that, in general, the greater the water content is above the liquid limit, the less viscous the flow.

The Plasticity Index (PI) is defined as the difference in the water contents of the soil at the liquid limit and the soil at the plastic limit. The PI is expressed as a whole number and provides an indication of how much water a soil can absorb during its time in the plastic state. Soils with high PIs will exhibit a high degree of volume change with changes in soil water content (Holtz and Kovacs, 1981).

Liquid and Plastic limit tests were conducted in general accordance with the appropriate ASTM procedure.

Resilient Modulus

The resilient modulus is an elastic modulus that is based on the recoverable strain of a material under repeated loads (Huang, 2004). Most of the materials used in pavement base and embankment construction are considered to be partially elastic and plastic. This means that the materials undergo some degree of permanent (plastic) deformation with each load. The elastic assumption is valid if the magnitudes of the applied loads are well below the ultimate strength of the material and the number of applied loads is large (Huang, 2004).

The resilient modulus tests were conducted in general accordance with standard TTI procedures.

Unconfined Compressive Strength

The compressive strength of a soil sample depends upon several factors. One factor is whether or not a confining pressure is applied to the test sample as the compressive load is applied. In general, the greater the confining pressure the greater the compressive strength of the sample. The confining pressure is often used to model the stress conditions of deep soil samples and obtain a more realistic assessment of in-place soil strength.

Another factor is what degree of sample deformation (strain) constitutes failure. For some embankment applications a strain of 5% or more may be acceptable, whereas a strain of 1% may be unacceptable for other applications. As such, a graph of compressive strength as it varies with percent strain is normally used to determine compressive strength in situations where the sample does not catastrophically fail.

The unconfined compression tests were conducted in general accordance with the appropriate ASTM procedure on samples that had already been subjected to resilient modulus testing. The use of the samples for both resilient modulus and unconfined compression testing is permissible because the resilient modulus test is considered to be a non-destructive test (Huang, 2004).

CHAPTER V
DRUM DEFLECTION COMPARED TO OTHER DATA

GENERAL

The roller drum deflection data was compared to data from several field and laboratory tests in an attempt to determine if a correlation existed between roller drum deflection and the level of compaction of the upper soil layer. The most common comparisons were with pFWD and FWD sensor deflection and dry unit weight measured with the nuclear gauge. Comparisons involving resilient modulus, unconfined compressive strength, and DCP penetration rate are not discussed in this chapter because the small amount of data available for comparisons precludes the development of statistically significant conclusions. However, the results of the resilient modulus tests are presented in the Chapter VII as a means to compare the starting and ending values of the elastic modulus for each layer.

The data presented below corresponds to pFWD, FWD, and unit weight readings taken in the test strips either before any passes where made with the RAM system or after several passes were made. In cases where the data was collected before any RAM passes were made, the roller drum deflection readings from the first test pass were used. In cases where the data was collected after several roller passes were made, the last set of roller drum deflection readings taken before the standard instrument tests were conducted was used.

REGRESSION ANALYSIS

Regression analysis is a method used to predict the value of a dependent characteristic, Y, given the value of an independent characteristic, X, (Revelle et al., 2004). Regression analysis requires a series of {X,Y} data pairs that are usually gathered from historical records, or laboratory/field experiments. The data pairs are plotted and the line through the data points that results in the lowest sum of the squared errors is deemed to be the best fit line. Error is defined as the difference between the

actual, measured value of Y for the corresponding measured value of X and the value of Y that would be found substituting the measured value of X into the equation of the best fit line (Scheaffer and McClave, 1990).

The slope of the best fit line can provide some insight into the interrelation or correlation of the test data. The closer the slope of the best fit line is to 0 the less useful the equation is to predict values of the dependent characteristic. The lack of usefulness is a result of the fact that for even large changes in the value of the independent characteristic, X, there is only a small change in the value of the dependent characteristic, Y, (Scheaffer and McClave, 1990; Revelle et al., 2004).

The dimensionless coefficient of determination, or R^2 is another tool available to judge whether or not the best fit line adequately models the data pairs. The R^2 value defines the amount of the variance in the dependent characteristic that is attributed to the regression equation. For example, an R^2 value of 0.61 would mean that 61% of the variance in the dependent characteristic is attributable to the regression equation. The remaining 39% of the variance is not attributable to the regression equation and is unexplained (Statpac, 2009). An R^2 value of 1 would mean that the best fit line passes directly through all of the data points and would suggest that a strong correlation exists between the independent and dependent characteristic (Scheaffer and McClave, 1990).

The RAM system was constructed to determine the compaction of the upper layer of the soil surface based on the deflection of the vibrating roller drum. As such, the data comparisons outlined below always use the roller drum deflection as the dependent characteristic. This convention was valid because the results of all other test methods such as pFWD and FWD sensor deflections were compared to roller drum deflection.

Correlation between the data sets would not prove that a causal relationship exists between the two test methods. However, correlation must be present in order for such a relationship to exist. In other words, if a correlation does not exist between the compared data points (i.e. low R^2 values), then there is not a causal relationship. A rigorous statistical analysis (t-distribution) of the data was not conducted because the

low R^2 values and the fact that the purpose of this dissertation is to discuss the development and testing of a mechanics based soil-roller interaction model.

pFWD SENSOR DEFLECTION

The pFWD measured the deflection of the ground surface at three points; immediately beneath the falling weight, and at distances of 30 cm (11.81 inches) and 60 cm (23.62 inches) from the first sensor. The sensors were labeled D1, D2, and D3 with sensor D1 located beneath the falling weight and sensor D3 located 60 cm (23.62 inches) from sensor D1. Sensors farther from the load point are more affected by deeper soils than sensors located closer to the load point (Lytton, 1989). The results of the comparison between roller drum deflection and pFWD sensors D1 and D3 are shown in Figures 5-1 and 5-2, respectively.

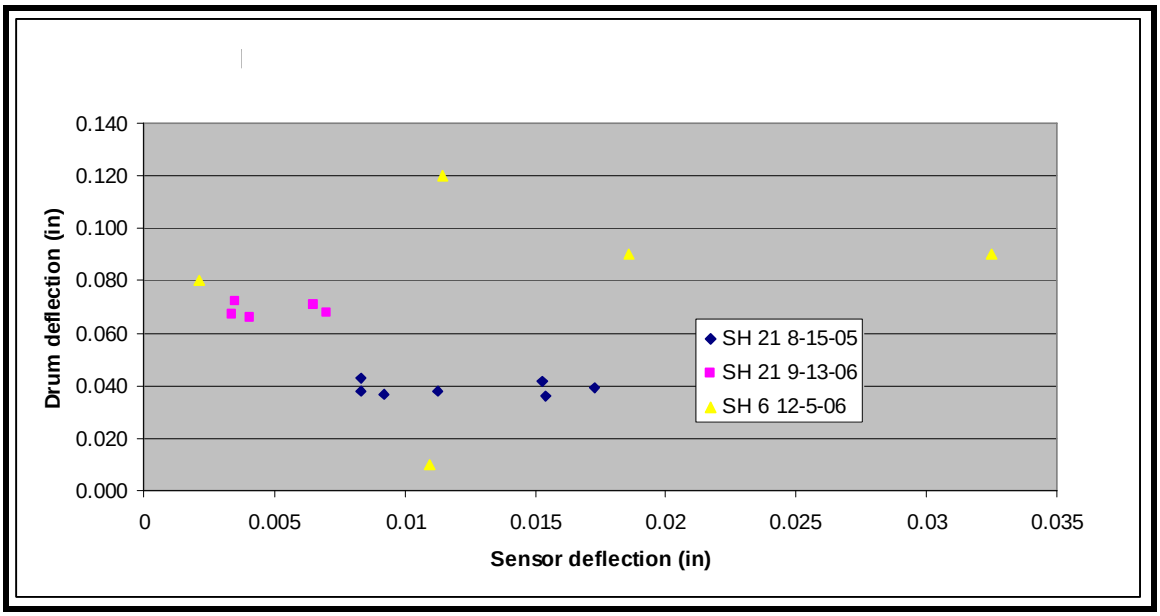

Fig. 5-1. pFWD sensor D1 deflection compared to drum deflection.

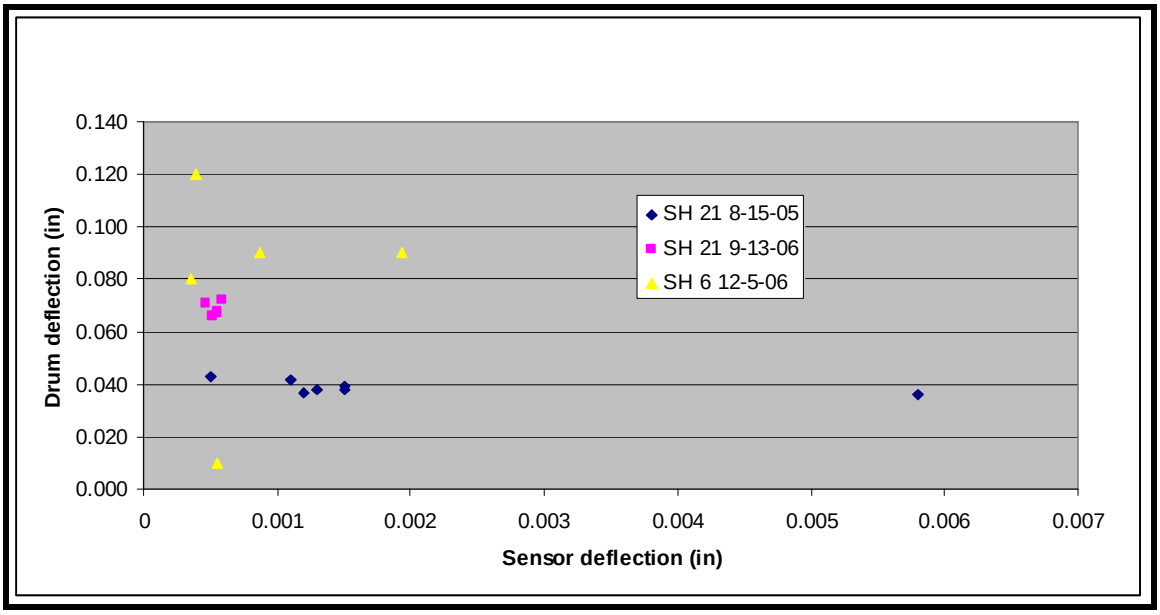

Fig. 5-2. pFWD sensor D3 deflection compared to drum deflection.

A visual comparison of the data presented in Figures 5-1 and 5-2 shows that the data taken on SH 21 in September 2006 has less scatter than the other 2 sets of data. Additionally, the SH 6 data has significant scatter for both sensors D1 and D3. The fact that the test strip was underlain with a synthetic geogrid may have contributed to the scatter. The R^2 values for a linear trend line for the 6 sets of data ranged from about 0.004 to 0.4. The low R^2 values indicated that the degree of correlation between roller drum deflection and pFWD sensor deflection was minimal, if any.

FWD SENSOR DEFLECTION

The FWD measured the deflection of the ground surface at 7 points; immediately beneath the falling weight, and 6 points spaced 12 inches (30.48 cm) perpendicular to the first sensor. The sensors were labeled R1 through R7 with sensor R1 located beneath the falling weight and sensor R7 located 72 inches (182.88 cm) from sensor R1. As with the pFWD, deflection of sensors farther away from the load point is governed more by the condition of the lower soil layers than the condition of the upper soil layers. The

results of the comparison between roller drum deflection and FWD sensors R1 and R7 are shown in Figures 5-3 and 5-4, respectively.

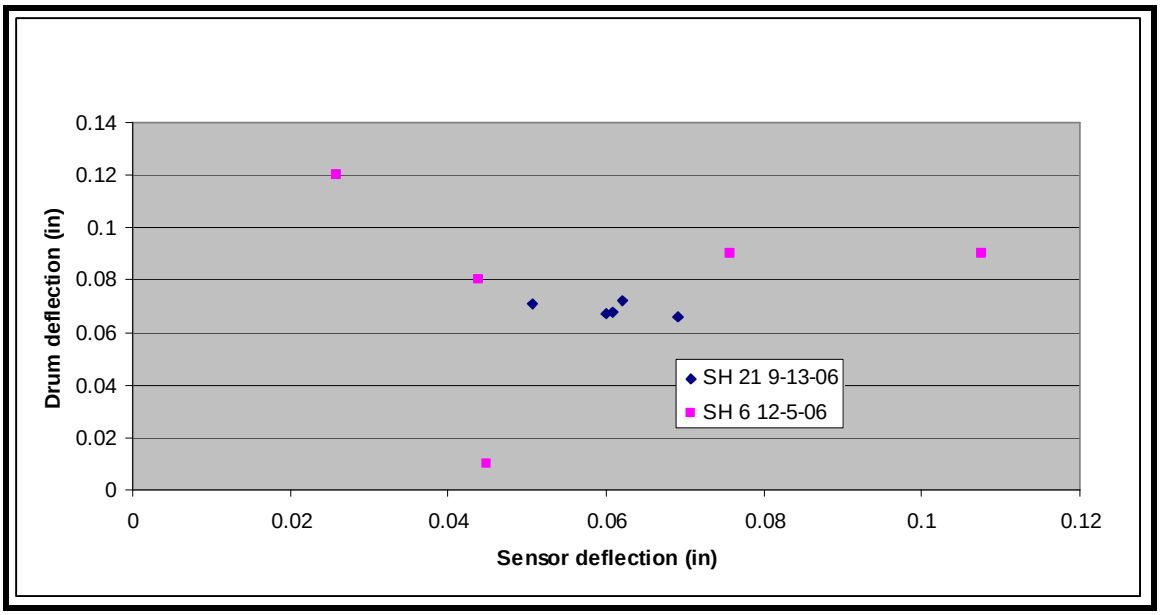

Fig. 5-3. FWD sensor R1 deflection compared to drum deflection.

Again, a visual comparison of the data presented in Figures 5-3 and 5-4 shows that the SH 21 data has less scatter than the SH 6 data. The R^2 values for a linear trend line through each of the 4 sets of data ranged from about 0.003 to 0.4. The low R^2 values suggest that whatever correlation that may exist between the data is weak, if any.

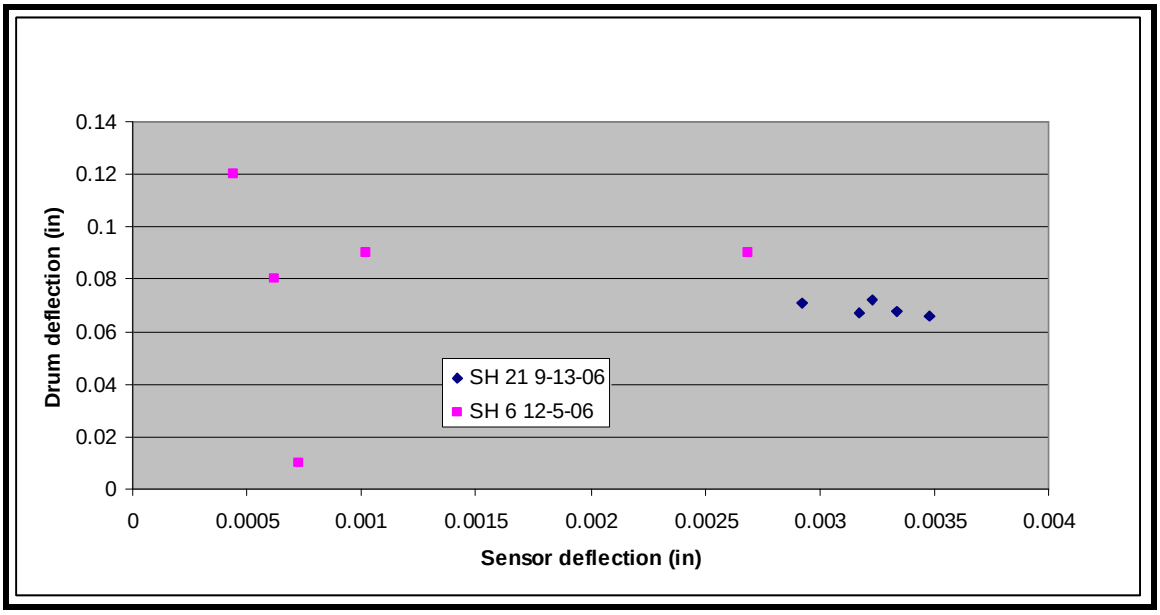

Fig. 5-4. FWD sensor R7 deflection compared to drum deflection.

FIELD DRY UNIT WEIGHT MEASUREMENTS

The dry unit weight of the upper 12-inches (30.48 cm) of material was measured with the nuclear gauge. The comparison between the roller drum deflection and the measured dry unit weigh is shown in Figure 5-5.

An examination of the data from the SH 21 testing, shown in Table 5-1, is enlightening. A roller drum deflection of 0.038 inches (0.965 mm) was measured for dry unit weights of 110.9 and 112.9 pcf (1,776.4 and 1,808.4 kg/m^3). In other words, the same roller drum deflection was measured for unit weights which varied by 2 pcf. Two pounds per cubic foot could easily be the difference between a soil meeting, or not meeting, specification. Additionally, dry densities ranging from 101.5 to 112.9 pcf (1,625.8 to 1,808.8 kg/m^3) corresponded to roller drum deflections within a narrow range of approximately 0.007 inches (0.1778 mm). Such inconsistent roller data is of little value in determining the dry density of the upper soil layer.

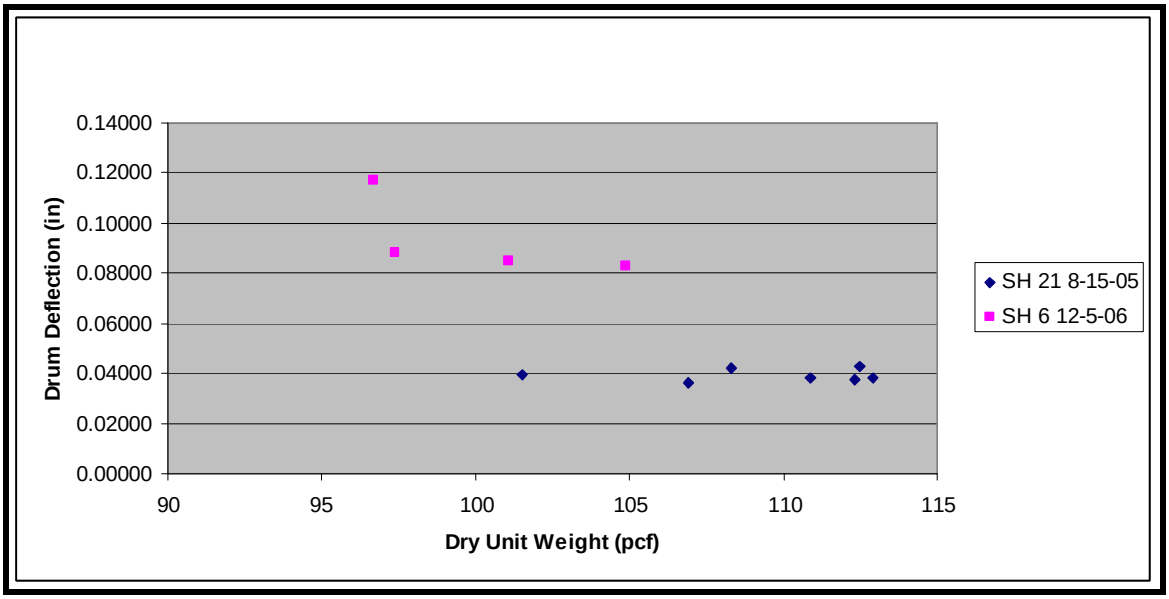

Fig. 5-5. Dry unit weight compared to drum deflection.

Table 5-1: SH 21 Dry Unit Weight vs. Roller Drum Deflection

Dry Unit Weight (pcf)	**Drum Deflection (in)**	**Dry Density (kg/m^3)**	**Drum Deflection (mm)**
101.5	0.039	405.0	0.991
106.9	0.036	426.5	0.914
108.3	0.042	432.1	1.067
110.9	0.038	442.5	0.965
112.3	0.037	448.1	0.940
112.5	0.043	448.9	1.092
112.9	0.038	450.5	0.965

The apparent lack of correlation was reinforced by the slopes and R^2 values of the regression equations for each data set. The slopes of the SH 6 and SH 21 regression equations were both very close to 0: -0.0017 and 0.00002, respectively. The R^2 value for SH 6 was 0.4182, and the R^2 value for SH 21 was 0.0016.

Further comparisons of the test data with the layer moduli inferred from the mechanics-based roller model will be made in Chapter VII.

CHAPTER VI
DERIVATION OF THE SOIL-ROLLER INTERACTION MODEL

GENERAL

As was shown in Chapter V, there was no evident correlation between the measured vibratory roller drum deflection and the degree of compaction within the upper soil layer. The lack of correlation was not surprising given the multitude of characteristics within the upper few feet of the soil system that can affect the deflection of the vibratory roller drum (density, water content, layer thickness, etc.). More importantly, correlation does not imply causation. Or simply: just because a reasonably well fit line can be drawn through a set of data points does not mean that the compared characteristics are actually interrelated. The subject soil-roller interaction model was derived through a mechanics based approach and then calibrated, not correlated, with available field and laboratory data.

BACKGROUND AND ASSUMPTIONS

The soil-roller interaction model developed for this dissertation (Figure 6-1) was an extension of work completed by Yoo and Selig (1979) and by Pietzsch and Poppy (1992). Their models were primarily developed as a way to theoretically evaluate proposed changes in roller design without the need to construct expensive physical prototypes. Neither of these earlier models allowed for consideration of multiple soil layers, nor rigorously addressed the non homogeneous nature of soil. The subject model contained 2 soil layers, but could be extended to 3 or more soil layers if circumstances warranted.

Model development began by separating the soil-roller system into 4 distinct sections. The first section was the roller frame, which contained the roller components that surround the roller drum and connect the drum to the remainder of the roller. The second section was the roller drum, including the rotating eccentric mass that causes the roller drum to vibrate. The third and fourth sections were the top and underlying soil

layers, respectively. The symbols used in the model are summarized in Table 6-1. Metric units were used during the model testing process because the majority of the available data regarding stiffness and damping were reported in metric units.

The free body diagrams (FBDs) for each of the 4 sections were constructed using the basic principles of statics and dynamics. The construction necessitated several simplifying, though realistic, assumptions. These assumptions are briefly explained in the following paragraphs. The FBDs of the model sections are included in the Appendix along with the detailed derivation of the model equations.

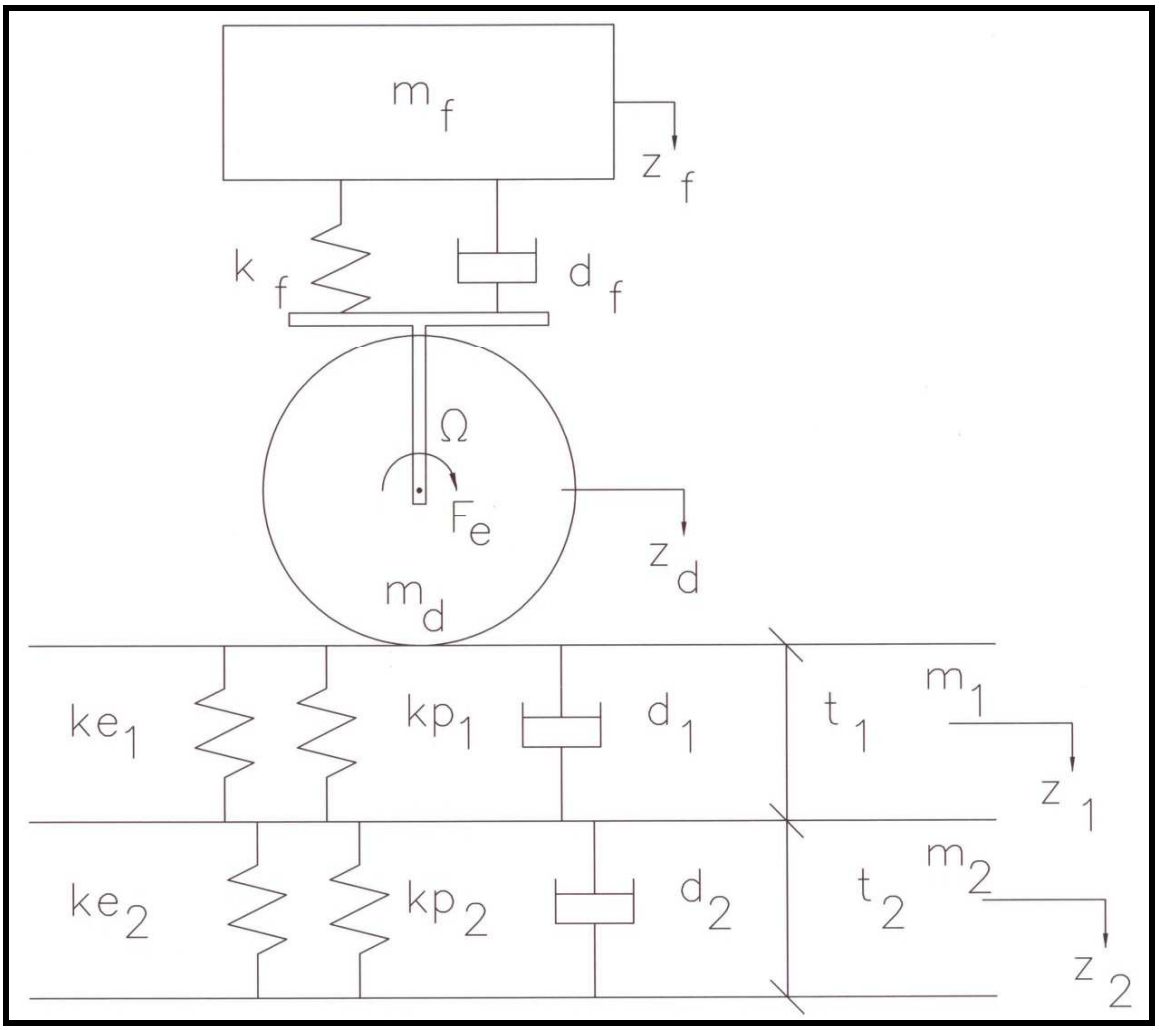

Fig. 6-1. Schematic of soil-roller interaction model.

Energy from the vibrating roller drum is imparted into the soil mass only when the roller drum is in contact with the soil surface. Therefore, the roller drum was assumed to be in contact with the soil surface throughout testing. Situations in which the roller drum was not in contact with the surface (i.e. the roller drum was double jumping) were not pertinent to this project and were not included in the model.

Table 6-1: Symbols Used in Soil-Roller Interaction Model

Symbol	**Description**	**Units**
m_f	mass of drum frame	mass
z_f	displacement of drum frame	length
k_f	elastic stiffness between drum frame and drum	force/length
d_f	damping between drum frame and drum	force*time/length
F_e	exciting force	force
$\Omega = \omega$	frequency of eccentric mass	Hertz or rad/sec
m_d	mass of drum	mass
z_d	displacement of drum	length
k_{e1}	elastic stiffness of top soil layer	force/length
k_{p1}	plastic stiffness of top soil layer	force/length
t_1	thickness of top soil layer	length
m_1	mass of the first soil layer	mass
d_1	damping of top soil layer	force*time/length
z_1	displacement of top soil layer	length
k_{e2}	elastic stiffness of lower soil layer	force/length
k_{p2}	plastic stiffness of lower soil layer	force/length
t_2	thickness of lower soil layer	length
m_2	mass of the second soil layer	mass
d_2	damping of lower soil layer	force*time/length
z_2	displacement of lower soil layer	length

When the roller drum is in contact with the ground surface the springs and dashpots are in compression. This means that the theoretical devices would push up on the elements above them (negative sign in the FBD) and downward on the elements below them (positive sign in the FBD). It may be useful to note here that springs are used to model resistance to displacement while dashpots are used to model resistance to the rate of displacement. In other words, springs resist movement while dashpots delay the motion.

The pertinent components acting on the roller frame are the mass of the frame, which can be estimated from manufacturer's data, and the isolating connections between the frame and the drum. The connections between the frame and drum were modeled with an elastic spring and a dashpot. The choice of an elastic spring was valid because the relative positions of the roller drum and roller frame are essentially equal at the beginning and end of operation. If the relative positions are not essentially equal, it would mean that the roller has suffered a mechanical failure.

The dashpot simulates the isolators present on the roller that minimize the amount of vibration transmitted from the vibrating roller drum to the remainder of the roller. If the dampers were not present the displacement of the roller frame would be nearly equal to or, depending on frequency, greater than that of the roller drum, which would result in damage to the roller and discomfort to the operator. The degree of damping can be estimated by attaching an accelerometer to the vibrating roller drum and a separate accelerometer to the roller frame. The difference between the 2 measured accelerations would be directly proportional to the effectiveness of the damping system (Rinehardt and Mooney, 2005).

The components acting on the roller drum are the rotating eccentric mass, the mass of the roller drum, both of which are available from manufacturer's data, the spring and dashpot connection from the roller frame, and the springs and dashpot of the top soil layer. The spring and dashpot between the roller drum and frame push up on the roller frame and down on the roller drum. Additionally, the elastic and plastic springs and

dashpot in the upper soil layer push up on the roller drum. The rotating eccentric mass is the driving force behind the model and is the primary component of compaction.

The rotating eccentric mass causes the roller drum to vibrate and allows the roller to impart dynamic, as well as, static energy into the soil mass. During operation, some of the energy causes the soil to densify and compact. Compaction is modeled with a plastic spring, which experiences a permanent deformation when the roller imparts enough energy to overcome the forces holding the soil particles apart. An elastic spring is necessary in each soil layer because not all imparted energy causes compaction. The stiffer, or more compact, that the soil matrix becomes the more of the imparted energy will be returned to the roller or passed through to the underlying layers (Anderegg and Kaufmann, 2004; Scullion et al., 2006; Thurner and Sandstorm, 2000). The dashpots in the soil layers model the energy absorbing characteristics of the soil layers.

DERIVATION OF THE MODEL

The starting point for the mechanics based soil-roller interaction model was Newton's Second Law of Motion which is stated as equation 6-1 (Sears et al., 1987):

$$F = M*A \qquad (6\text{-}1)$$

where F = force, N or kN

M = mass, kg

A = acceleration, m/sec^2

By combining Newton's Second Law with the free body diagram developed for each of the model's 4 sections, base or starting equations were developed. The notation used in the equations was summarized in Table 6-1. Additionally, prime and double prime (′ and ″) following a displacement, z, denote velocity and acceleration of the particular component. For example, z'_f denotes velocity of the roller frame and z''_f denotes the acceleration of the roller frame.

The base equation for the roller frame is stated in equation 6-2:

$$m_f(z''_f) = -k_f(z_f-z_d)-d_f(z'_f-z'_d) \quad (6\text{-}2)$$

The base equation for the roller drum is stated in equation 6-3:

$$m_d(z''_d) - F_e = k_f(z_f-z_d)+d_f(z'_f-z'_d)-k_{e1}(z_d-z_1)-k_{p1}(z_d-z_1)-d_1(z'_d-z'_1) \quad (6\text{-}3)$$

The base equation for the top soil layer is stated in equation 6-4:

$$m_1(z''_1) = k_{e1}(z_d-z_1)+k_{p1}(z_d-z_1)+d_1(z'_d-z'_1)-k_{e2}(z_1-z_2)-k_{p2}(z_1-z_2)-d_1(z'_1-z'_2) \quad (6\text{-}4)$$

The base equation for the second soil layer is stated in equation 6-5:

$$m_2(z''_2) = k_{e2}(z_1-z_2)+k_{p2}(z_1-z_2)+d_2(z'_1-z'_2) \quad (6\text{-}5)$$

A detailed derivation of the model equations is included in the Appendix. However, a test of the initial validity of equations 6-2 through 6-5 can be made by ensuring the dimensional consistency of each of the term groupings, which should have units of force or mass*length/time^2. For example, the left hand side of equation 6-2 is the product of mass and acceleration, which is force. The first grouping of terms on the right hand side of the equation is the product of stiffness (force/length) and displacement (length). The lengths cancel out, which leaves force. The second grouping of terms is the product of damping (force*time/length) and velocity (length/time). The time and length terms cancel out, which also leaves force. Thus, the units of all of the term groupings on the left and right hand sides of the equations are force. Analysis of the remaining equations yielded similar results.

The force causing the roller drum to vibrate was an eccentric, rotating mass, which produced a varying load upon the soil. As such, the displacements, velocities and

accelerations within each of the 4 base equations, which depended upon the force exerted by the drum, needed to be expressed in terms of the rotational frequency, Ω or ω of the load. Additionally, the dampers between the roller drum and the roller frame, and the damping of each soil layer, caused the load transmission through the roller frame and soil mass to lag behind the rotating mass. To account for this phenomenon a lag angle, Φ was introduced into the base equations for the roller frame and the first and second soil layers.

The new terms for displacement, velocity and acceleration were then substituted into equations 6-2 through 6-5. The equations were then expanded, similar terms were gathered and the equations were simplified. A matrix was developed and the determinants and discriminants were calculated. Four equations showing the displacement of the roller drum, roller frame, upper soil layer and second soil layer were developed.

The final equation describing the displacement of the roller frame is stated in equation 6-6:

$$X1 = -F_e A12[(A33A44)-(A34A43)+(A23A34)-(A23A44)] \div A11[(A22A33A44)-(A22A34A43)+(A23A34A42)-(A23A32A44)] -A12[(A21A33A44)-(A21A34A43)-(A23A34A41)-(A23A31A44)] \quad (6\text{-}6)$$

The final equation describing the displacement of the roller drum is shown in equation 6-7:

$$X2 = F_e A11[(A33A44)-(A34A43)+(A23A34)-(A23A44)] \div A11[(A22A33A44)-(A22A34A43)+(A23A34A42)-(A23A32A44)] -A12[(A21A33A44)-(A21A34A43)-(A23A34A41)-(A23A31A44)] \quad (6\text{-}7)$$

The final equation describing the displacement of the top soil layer is stated in equation 6-8:

$$X3 = F_eA11[(A22A44)-(A22A34)+(A34A42)-(A32A44)] - F_eA12[(A21A44)-(A21A34)+(A34A41)-(A31A44)] \div A11[(A22A33A44)-(A22A34A43)+(A23A34A42)-(A23A32A44)] - A12[(A21A33A44)-(A21A34A43)-(A23A34A41)-(A23A31A44)] \quad (6\text{-}8)$$

The final equation describing the displacement of the second soil layer is stated in equation 6-9:

$$X4 = F_eA11[(A22A33)-(A22A43)+(A23A42)-(A23A32)+(A32A43)-(A33A42)]-F_eA12[(A21A33)-(A21A43)+(A23A41)-(A23A31)+(A31A43)-(A33A41)] \div A11[(A22A33A44)-(A22A34A43)+(A23A34A42)-(A23A32A44)] - A12[(A21A33A44)-(A21A34A43)-(A23A34A41)-(A23A31A44)] \quad (6\text{-}9)$$

Where $X1=Z_fe^{-i(\omega t-\Phi f)}$

$X2=Z_de^{-i\omega t}$

$X3=Z_1e^{-i(\omega t-\Phi 1)}$

$X4=Z_2e^{-i(\omega t-\Phi 2)}$

$A11=(-m_f\omega^2+k_f-d_fi\omega)$

$A12=(-k_f+d_fi\omega)$

$A13=0$

$A14=0$

$A21=(-m_f\omega^2)$

$A22=(-m_d\omega^2+k_{e1}+k_{p1}-i\omega d_1)$

$A23=(-k_{e1}-k_{p1}-i\omega d_1)$

$A24=0$

$A31=(-m_f\omega^2)$

$A32=(-m_d\omega^2)$

$A33=(-m_1\omega^2+ke2+k_{p2}-i\omega d_2)$

$A34=(-ke2-k_{p2}-i\omega d_2)$

$A41=(-m_f\omega^2)$

$A42=(-m_d\omega^2)$

$A43=(-m_1\omega^2)$

$A44=(-m_2\omega^2)$

$i=(-1)^{1/2}$

CHAPTER VII
TESTING OF THE SOIL-ROLLER INTERACTION MODEL

GENERAL

Testing of the model described in Chapter VI was conducted using field and laboratory data obtained during the development and testing of the RAM system. The testing methodology consisted of determining initial input values for the 14 characteristics comprising the model, performing a sensitivity analysis on the 14 characteristics, modifying the 8 characteristics related to the stiffness and damping of the soil layers to minimize the difference between the measured and calculated roller drum deflection and comparing the initial soil input characteristic values to the values needed to minimize the difference between the measured and calculated roller drum deflections. The model would be considered to be an accurate prediction of the degree of compaction of the upper soil layer if the calculated roller deflection matched the measured roller deflection to within approximately 1%.

MODEL TESTING

Expansion of the 4 base equations, 6-2 through 6-5, resulted in 4 equations, 6-6 through 6-9, which described the displacement of the 4 components of the model; roller frame, roller drum, top soil layer and second soil layer. The field testing of the RAM system measured the acceleration of the roller drum. The displacement of the roller drum was calculated in the field by double integrating the measured acceleration. The accelerations of the other 3 components of the model; roller frame, top soil layer and second soil layer, were not measured. Therefore, the model was tested by using Equation 6-7, which described the displacement of the roller drum.

An Excel spreadsheet was developed to test the model. The model contained 14 input characteristics. Six of the characteristics described the roller and 8 characteristics described the first and second soil layers. The data used to test the model came from the

field testing conducted on SH 21 on August 18, 2005 and the results of laboratory tests conducted on soil samples taken from this site.

The initial value of a number of the characteristics relating to the mass, stiffness and damping of the soil layers varied at each of the 6 points tested within the test strip. The variation was caused by the fact that the measured soil density, modulus and layer thickness at each of the 6 test points was not consistent. The approximate initial input characteristics used in the testing, and the source of each characteristic, are summarized in Table 7-1.

Table 7-1: Initial Values of Input Characteristics Used for Model Testing

Input Characteristic	**Value (units)**	**Source**
m_f	1,346 (kg)	Caterpillar, 2003; Pietzsch and Poppy, 1992
k_f	5,480,000 (N/m)	Pietzsch and Poppy, 1992
d_f	10,480 (N*s/m)	Pietzsch and Poppy, 1992
F_e	105,000 (N)	Caterpillar, 2003; Pietzsch and Poppy, 1992
$\Omega = \omega$	200.43 (radians/s)	Caterpillar, 2003
m_d	2,046 (kg)	Caterpillar, 2003; Pietzsch and Poppy, 1992
k_{e1}	33E6 to 66E6 (N/m)	Pietzsch and Poppy, 1992; Richart et al., 1970
k_{p1}	29E6 to 57E6 (N/m)	Pietzsch and Poppy, 1992; Richart et al., 1970
m_1	215 to 1,456 (kg)	Field and laboratory measurements
d_1	7.8E3 to 21E3 (N*s/m)	Richart et al., 1970; Tateyama et al., 2006
k_{e2}	39E6 to 140E6 (N/m)	Pietzsch and Poppy, 1992; Richart et al., 1970
k_{p2}	33E6 to 122E6 (N/m)	Pietzsch and Poppy, 1992; Richart et al., 1970
m_2	886 to 2,147 (kg)	Field and laboratory measurements
d_2	15E3 to 39E3 (N*s/m)	Richart et al., 1970; Tateyama et al., 2006

SELECTION OF THE INITIAL MODEL INPUT VALUES

The initial values for several of the model characteristics were easily obtained from manufacturer's literature and/or field and laboratory measurements. Other characteristics, particularly those relating to the damping and stiffness of the soil layers, were inter-related to the shear modulus of the soil layer and were more difficult to determine. The following subsections describe the procedures and assumptions used to find the initial values for each of the 14 input characteristics.

It bears reiterating at this point that the RAM system was primarily developed as a quality assurance tool. As such, the soil input characteristics used to validate the model were taken from test points that had reportedly met project specifications relating to density and water content prior to TTI's testing. Uncompacted, loose or excessively dry soil could have vastly differing values for mass, shear modulus, stiffness and damping than soil that has been compacted to at or near its specified unit weight.

Mass of the Roller Drum (m_d) and Mass of the Roller Frame (m_f)

The mass of the roller drum (m_d) term accounts for the mass of the roller drum and the components housed inside the drum that provide the excitation force which causes the roller to vibrate.

The manufacturer's data for the CS-433E Caterpillar roller that was used in the RAM system testing stated that the total operating weight of the roller was 6,745 kg (14,875 lbs) and that the operating weight at the drum was 3,410 kg (7,515 lbs) (Caterpillar, 2003). These weights were very similar to the weights of the HAMM 2310 roller used by Pietzsch and Poppy during their research in the late 1980's and early 1990's (Pietzsch and Poppy, 1992). The similarities between the rollers suggested that a reasonably accurate value of m_d could be obtained by adjusting the Pietzsch and Poppy value of m_d by the ratio of the weight of the HAMM 2310 roller drum to the weight of the CS-433E roller drum.

The mass of the roller frame (m_f) term encompasses the mass of the roller super structure that surrounds and supports the roller drum and connects the drum to the

remainder of the roller body. This mass is separated from the roller drum by several isolation pads, which decrease the vibrations transmitted to the frame and the remainder of the roller. Pietzsch and Poppy found their roller frame mass by subtracting the mass of the roller drum from the static weight of the roller at the drum reported by the manufacturer. This procedure was judged to be adequate for the subject model based on the similarities between the rollers.

Angular Frequency of the Eccentric Mass (ω or Ω)

The vibration of the roller drum is the result of the rapid rotation of an eccentric mass contained in the roller drum. The angular frequency (ω) indicates how many times the eccentric mass rotates through 360 degrees in a second. The model requires that the angular frequency be inputted in radians per second. The manufacturer's data stated that the vibrating frequency of the roller was 31.9 hertz, which equates to approximately 200 radians per second (Caterpillar, 2003). Drum acceleration data obtained during field testing confirmed that the eccentric mass rotated at approximately 32 hertz.

Frame Stiffness (k_f)

The frame stiffness term (k_f) models the resistance to displacement between the roller drum and the roller frame. The frame stiffness is an elastic stiffness in that essentially all of the displacement that occurs between the roller drum and roller frame resulting from the vibration of the roller drum is recovered once the vibrations cease. If the displacement was plastic, or non-recoverable, then a permanent, ever increasing deformation between the roller drum and roller frame would occur during operation.

Pietzsch and Poppy (1992) used a value of 5,480,000 N/m for the HAMM 2310 roller. This value was judged to be acceptable as an initial value for the roller model because of the reported similarities with the CS 433E roller.

Frame Damping (d_f)

The isolation mounts that are located between the roller drum and the roller frame are installed to reduce, or damp, the transfer of vibrations between the roller drum and the remainder of the roller. Excessive vibrations within the roller would stress the mechanical systems and cause discomfort to the operator. According to research by others, isolation mounts typically prevent approximately 90% of the drum vibrations from reaching the roller frame (Rinehart and Mooney, 2005).

A frame damping value of 10,480 N*s/m was used for the HAMM 2310 roller by Pietzsch and Poppy (1992). Again, this value was judged to be acceptable as an initial value for the roller model.

Force Applied by Rotating Eccentric Mass (Fe)

The roller drum vibrations are produced by a rotating eccentric mass housed within the central portion of the drum (Caterpillar, 2003). The dynamic loading caused by the vibrations imparts energy into the underlying soil mass and contributes to compaction. The manufacturer's data indicated that the roller produced between 67,000 N and 134,000 N of centrifugal force when operating at 31.9 hertz (Caterpillar, 2003). An initial value of Fe of 105,000 N was selected based on the Pietzsch and Poppy (1992) testing.

Mass of the Soil Layers (m_1 and m_2)

The purpose of the model was to determine the degree of compaction of the top soil layer by monitoring the displacement of the vibrating roller drum. However, in order to test the accuracy of the model by comparing the measured roller drum displacement to the calculated roller drum displacement, the masses of the first and second soil layers (m_1 and m_2) had to be input into the model. Should the model prove to be accurate the model equation could be rearranged to solve for m_1.

Determination of the masses required several steps. First, the wet and dry unit weights of the Shelby tube soil samples taken from each layer were found. Once the unit

weights were found they were converted into wet and dry unit masses. Next, the depth of the first and second soil layers had to be determined. The depth of the first soil layer was estimated by finding the change in the dynamic cone penetrometer (DCP) penetration rate at each point. The depth at which the penetration rate, measured in blows per inch, changed was assumed to represent the boundary between soil layers. The effective depth of the DCP was approximately 30 inches and none of the 6 points within the test section showed a second change in penetration rate that would have denoted the boundary between the second and third soil layer. Research by others suggested that the limiting depth of compaction for a roller such as the CS 433E was approximately 1 meter (3.28 feet) (Richart et al., 1970; Rinehart and Mooney, 2009). The thickness of the second layer was assumed to be the difference between 1 meter and the thickness of the first soil layer.

The volume of soil within each layer that was potentially subject to compaction was estimated. The vibrating roller drum is essentially a vibrating machine sitting atop the soil. The design of foundations for vibrating machines tends to model the dissipation of vibration energy into the underlying soil as an inverted cone (Wolf, 1994; Wolf and Deeks, 2004). A dissipation rate of 2:1 was assumed within the soil mass. This meant that the cone of dissipation increased horizontally 0.3 m (1 foot) for every 0.6 m (2 feet) of vertical penetration into the soil mass. A 0.15 m (6 inch) roller contact surface was assumed based on observations made during field testing with the roller. The manufacturer's literature reported that the roller drum was 1.7 m (5.58 feet) long. The mass of soil within the first and second soil layers at each point were then calculated based on the layer thickness, vibration dispersion geometry and measured unit masses at each of the 6 test points.

Soil Elastic Stiffness Characteristics (ke_1 and ke_2)

The elastic stiffness characteristics (ke_1 and ke_2) model the portion of the soil matrix that is not permanently deformed by the passage of the vibrating roller. The more compact, or denser, that the soil matrix becomes the less the soil deformations when the

roller passes and the more energy is rebounded back toward the roller (Pietzsch and Poppy, 1992; Anderegg and Kaufmann, 2003).

Very little data regarding elastic spring constants of soil undergoing compaction was found in the literature. As such, techniques used to estimate the elastic spring constants of soil beneath vibrating machinery were used. These techniques were judged to be adequate because the goal of machine foundation design is to minimize movement of the foundation so that the operation of the machine is not compromised. Because the RAM system was designed as a QA system, the tested soil had reportedly met density specification and should experience minimal permanent, or plastic, deformation when the roller was driven across.

Richart et al., (1970) devoted several sections of their book Vibrations of Soil and Foundations to estimating elastic spring constants of soil based on the shear modulus of the soil mass. The soil at the test points had been tested by a portable falling weight deflectometer, or pFWD. Back calculation of the deflection bowl data produced by the pFWD with the manufacturer's software yielded 3 elastic moduli at each test point. The farther away the soil surface deflection detector is from the drop point, or center of the pFWD, the less influence the upper soil layers have on the deflection, and by extension the modulus (Lytton 1989; Scullion et al., 1989). As such, the modulus related to the deflection beneath the pFWD pad was used as the layer 1 modulus while the modulus related to the deflection beneath the third pFWD sensor was used as the layer 2 modulus.

Richart et al., (1970) provided a formula relating the elastic modulus to the shear modulus, which is stated below as equation 7-1:

$$G = E/(2*(1+v)) \qquad (7\text{-}1)$$

where G = shear modulus, N/m^2

E = elastic modulus, N/m^2

v = Poisson's ratio

The literature generally reports the range of Poisson's ratios of clay soil, which was the soil type present at the test site, to be between 0.3 and 0.5 (Holtz and Kovacs, 1981; Richart et al., 1970; Das, 2008). A mid-range value of 0.4 was judged to be acceptable for model analysis given that this value is commonly used in foundation design of vibrating machines (Richart et al., 1970).

Once the shear modulus within each layer was determined with equation 7-1 the information could be used to determine the starting values of the elastic spring constants by the following equation, 7-2 (Richart et al., 1970):

$$k_e = (4*G*r_0)/(1-v) \qquad (7\text{-}2)$$

where G = shear modulus, N/m2

r_0 = the radius of an equivalent circular area of roller drum contact, m

v = Poisson's ratio

The contact area of the roller drum used during testing was estimated to be approximately 0.15m by 1.7m (0.5 ft by 5.6 ft), which corresponded to a narrow footing with a very long length. The charts provided in the literature to estimate the spring constants of a rectangular foundation were not useful because machine foundations are typically not 11 times longer than they are wide. To work around this difficulty, the roller drum contact area of approximately 0.26 m^2 (2.8 ft^2) was transformed into an equivalent circular area with a radius of approximately 0.3 m (1 ft). A Poisson's ratio of 0.4 was still used.

Equation 7-2 points out that the elastic spring constant depends upon the radius, or size of the loaded area. As such, the spring constant will vary as compaction continues because the contact area of the roller drum generally decreases as compaction progresses. In essence, the roller drum walks its way out of the fill as the fill gets denser and stronger and needs less area to support the weight of the roller.

The elastic modulus values obtained from the pFWD tests that were used to determine the shear moduli and elastic spring constants at each point are summarized in Table 7-2.

Table 7-2: Initial Moduli and Elastic Stiffness Values

Point	Layer	E (N/m^2)	G (N/m^2)	k_e (N/m)
1	1	46,666,667	16,666,667	33,333,334
1	2	68,333,333	24,404,762	48,809,524
2	1	61,500,000	21,964,286	43,928,571
2	2	90,333,333	32,261,905	64,523,809
3	1	52,500,000	18,750,000	37,500,000
3	2	54,666,667	19,523,810	39,047,619
4	1	69,500,000	24,821,429	49,642,857
4	2	65,500,000	23,392,857	46,785,714
5	1	85,500,000	30,535,714	61,071,429
5	2	79,000,000	28,214,286	56,428,571
6	1	92,000,000	32,857,143	65,714,286
6	2	196,000,000	70,000,000	140,000,000

Soil Plastic Stiffness Characteristics (kp_1 and kp_2)

The plastic stiffness characteristics (kp_1 and kp_2) model the portion of the soil matrix that is permanently deformed, or compacted, by the passage of the vibrating roller. The plastic springs essentially lock into place as the soil is compacted. Further compaction of the soil takes place only if subsequent loads cause the numerically stiffer elastic springs to deflect more than they have during the previous loadings (Pietzsch and Poppy, 1992).

As with the elastic springs, very little data regarding plastic spring constants of soil undergoing compaction was found in the literature. Foundation design data was not helpful because foundations are supposed to be designed to keep the soil in the elastic rather than the plastic region. The Pietzsch and Poppy (1992) soil-roller model used a value of 75.8 x 10^6 N/m for their plastic spring constant, which was 13% lower than the corresponding value of their elastic constant. This 13% reduction relationship was used to set the initial values of the plastic spring constants at each of the 6 test points.

Soil Damping Characteristics (d_1 and d_2)

Damping serves to decrease motion once a displacement has occurred. For example, stiffness is what makes it difficult to stretch a coiled spring. However, once a spring is stretched and released it will continue to oscillate unless damping is present to attenuate and eventually halt the oscillation.

There are 2 types of damping that are applicable to the subject model; material damping and geometric damping. Material damping depends upon the composition of the material. For example, rubber damps vibrations better than steel, which is why rubber is often used as a vibration isolator between steel components. Geometric damping depends on the shape or amount of the material. Rubber isolation mounts with a few grams of mass would generally be less effective at damping vibrations than isolation mounts with a few kilograms of mass. No attempt was made to separate the individual contributions of each type of damping within the model.

More data was found in the literature relating to soil damping than was found relating to the elastic and plastic stiffness characteristics. However, much of the data was related to the design of large foundations rather than to compacting soil (Richart et al., 1970; Wolf, 1994; Wolf and Deeks, 2004). Tateyama et al., (2006) used a formula similar to equation 7-3 to calculate their damping values:

$$d = 2*D*(m*k_e)^{0.5} \quad (7\text{-}3)$$

where d = the combined material and geometric damping of the material, N*s/m

D = a dimensionless material damping factor

m = the mass of the material causing the damping, kg

k_e = the elastic stiffness of the material causing the damping, N/m

The value of D selected for the model was 0.035, which was the average value for material damping reported in the literature for clay soils (Richart et al., 1970).

The values used to obtain the initial input values for the damping at each of the 6 test points are summarized in Table 7-3.

Table 7-3: Initial Mass, Elastic Stiffness and Damping Values

Point	Layer	Mass (kg)	k_e (N/m)	d (N*s/m)
1	1	383.3	33,333,334	7912
1	2	1833.6	48,809,524	20,941
2	1	638.4	43,928,571	11,722
2	2	1618.8	64,523,809	22,623
3	1	934.3	37,500,000	13,103
3	2	1327.8	39,047,619	15,939
4	1	255.6	49,642,857	7885
4	2	2040.9	46,785,714	21,630
5	1	1456.0	61,071,429	20,874
5	2	886.3	56,428,571	15,654
6	1	215.1	65,714,286	8322
6	2	2147.7	140,000,000	38,384

INITIAL RESULTS

A roller drum displacement was calculated for each of the 6 test points using the initial values of the 14 input characteristics described in the subsection above. The

calculated value of roller drum displacement was then compared to the measured value of roller drum displacement at each point. The measured value of roller drum deflection was deemed to be the correct value. Therefore, a negative percent difference would indicate that the calculated value of roller drum deflection was less than the measured value. A summary of the measured and calculated values of roller drum deflection, and the percent difference between the measured and the calculated values, is presented in Table 7-4.

Table 7-4: Roller Drum Deflections and Differences Using Initial Estimates

Point	Measured Roller Drum Deflection (m)	Calculated Roller Drum Deflection (m)	Percent Difference
1	0.001	0.01034	934.3
2	0.00107	0.00095	-10.8
3	0.00091	0.00245	169.7
4	0.00096	0.00274	185.7
5	0.00108	0.00006	-94.5
6	0.00095	0.00010	-89.0

SENSITIVITY ANALYSIS OF MODEL ERROR

The initial results summarized in Table 7-4 were based on estimated values for the input characteristics. A sensitivity analysis was conducted on the 14 input characteristics to determine which characteristics most greatly influenced the model error, or difference between the measured and calculated values of roller drum deflection. Each of the 14 input characteristics were individually increased and then decreased by 10% of the initial input value. The sensitivity coefficient for each characteristic was then determined by comparing the change in percent error to the percent change in the initial value of each characteristic, which was a constant ±10 %.

For example, when the mass of the roller drum (m_d) was increased by 10% the difference at Point 2 decreased from -10.8% to -3.6%. When the mass of the roller drum at Point 2 was decreased by 10% the difference at Point 2 increased from -10.8% to -16.9%. The absolute value of the change in differences resulting from the increase and decrease in the initial value was 13.3%. The 13.3% was then divided by the absolute value of the initial percent difference, -10.8%, which resulted in a value of 1.23. Dividing 1.23 by 20% yielded a sensitivity coefficient of approximately 6.16.

The higher the sensitivity coefficient of an individual characteristic, the greater the effect that changes in that characteristic have on the outcome of the formula. The sensitivity coefficient for the frequency of the vibrating mass within the roller drum (ω) at Point 2 was 89.17. This means that the model error is approximately 14.4 times more sensitive to changes in frequency than it is to changes in the mass of the roller drum at Point 2. As such, it is about 14.4 times more important to accurately determine the angular frequency than it is to determine the mass of the roller drum at Point 2.

The average values of the sensitivity coefficients of each input characteristic at all 6 test points were calculated and then rank ordered from highest to lowest. Relatively small changes in the characteristics with the highest sensitivity characteristics would affect the model error more than corresponding changes in the values of input characteristics with the lowest sensitivity coefficients. The average values of the sensitivity coefficients, in descending order, are contained in Table 7-5.

Interpretation of Sensitivity Analysis

The following subsections provide an interpretation of the model error sensitivity analysis for each of the 14 input characteristics using the average sensitivity coefficients shown in Table 7-5.

Table 7-5: Average Model Error Sensitivity Coefficients

Characteristic	Average Sensitivity Coefficient
ω	36.88
ke_1	8.9
m_2	8.18
ke_2	5.23
m_d	4.14
kp_1	3.96
kp_2	2.28
Fe	2.12
k_f	1.10
m_1	0.47
m_f	0.11
d_2	0.11
d_f	0.07
d_1	0.02

Angular Frequency (ω)

By rank ordering the sensitivity characteristics it becomes readily apparent that the angular frequency plays a key role in the model error. In fact, the model error is approximately 17 times less sensitive to changes in the eccentric force (Fe) than to changes in angular frequency. Fortunately, the eccentric mass reached its top speed within a few seconds of being activated and does not significantly vary during operation (Caterpillar, 2003). The field measurements of angular frequency matched closely with the value of 31.9 hertz reported in the manufacturer's literature. As such, confidence is high that the correct value of angular frequency was input into the model.

Soil Layer Masses (m_1 and m_2)

The model error is apparently, on average, 17 times more affected by changes in the mass of the second soil layer than to changes in the mass of the top soil layer. This characteristic can be highly undesirable because it is ultimately the mass of the top soil layer that needs to be known to determine the degree of compaction under most current standard specifications (Spangler and Handy, 1982; TxDOT, 2005). The mass, or degree of compaction, of the second soil layer, is of much less importance during the construction process because that layer must meet specifications before the next layer can be added.

Soil Layer Stiffnesses (ke_1, ke_2, kp_1 and kp_2)

The model error is approximately 2 times more sensitive to changes in the elastic stiffnesses as it is to changes in the plastic stiffnesses. This result is not surprising because the plastic stiffnesses are calculated as a fraction of the elastic stiffnesses. Additionally, the soil layer damping characteristics (d_1 and d_2) depend on the elastic stiffnesses, as well as the mass of the soil layers (m_1 and m_2). The intertwining of the elastic stiffnesses with several other characteristics means that small changes in the elastic stiffnesses will telegraph through to other characteristics and ultimately have a more pronounced affect on the model.

Roller Components (m_d, m_f, k_f and d_f)

The model error is apparently least sensitive to changes in the amount of damping between the roller drum and the roller frame and the mass of the roller frame. This is not surprising because the acceleration of the roller drum was measured during the field testing procedures. The damping between the roller drum and the roller frame, the stiffness of the roller frame and the mass of the frame, would probably have been more important if the acceleration of the roller frame been measured and used to test the model.

The average sensitivity coefficient of the mass of the roller drum was approximately 4 times higher than the sensitivity coefficient for the stiffness of the roller frame and almost 60 times higher than the mass of the roller frame. As such it is fairly important to have a good estimate of the roller drum mass to input into the model. Fortunately, information regarding the mass of the roller drum, and the other roller related characteristics, could be obtained from a detailed study of the roller and/or from the manufacturer. Once the values of the inputs are found they would not appreciablely change during the lifetime of the roller.

Magnitude of the Eccentric Force (Fe)

The eccentric force is the main source of soil compaction and the driving force behind the model. The roller drum would not vibrate without the eccentric mass rotating and dynamic energy would not be imparted into the soil to be reflected back to the roller and detected by the accelerometer. As with the mass of the roller drum (m_d), a good estimate of the eccentric force could be obtained from the manufacturer for various combinations of roller drum amplitude and frequency.

Soil Damping (d_1 and d_2)

The model error was apparently less sensitive to changes in the soil layer damping characteristics than it was to changes in the mass of the corresponding soil layer. For example, the model error was almost 75 times more sensitive to changes in the mass of the second soil layer (m_2) than to changes in the damping of layer 2. The model was about 24 times as sensitive to changes in the mass of the first soil layer (m_1) compared changes in the damping of the first soil layer. The suggestion that the damping of layer 2 plays a larger role in the outcome of the model than the damping of layer 1 may be the result of the generally greater volume of the second soil layer, and hence geometric damping, than of layer 1.

SENSITIVITY ANALYSIS OF THE MODEL

The previous section outlined how the sensitivity of the model error was found by comparing the calculated value of roller drum deflection with the measured value of roller drum deflection. The current section deals with determining the sensitivity of the model to changes in the input characteristics. The model sensitivity was analyzed by adjusting each of the 14 input characteristics up and down by 10% from their starting values. The value of roller drum deflection that resulted from each of the changes in the input characteristics was then compared to the initial calculated value of roller drum deflection at the appropriate test point. The average model sensitivity coefficients for all 6 test points are shown in Table 7-6.

It is apparent that the magnitudes of the model error sensitivity coefficients have similar magnitudes as the model sensitivity coefficients, as shown in Table 7-7. For example, the angular frequency had a model error sensitivity coefficient of 36.88 while the angular frequency had a model sensitivity coefficient of 26.39. Additionally, the sensitivity coefficients of the roller and soil damping characteristics were all well below 1. The rank order of the coefficients remained very similar between the two analyses, as shown in Table 7-8.

Table 7-6: Average Model Sensitivity Coefficients

Characteristic	Average Sensitivity Coefficient
ω	26.39
ke_1	7.62
m_2	7.17
ke_2	3.79
kp_1	3.48
Fe	2.12
m_d	1.76
kp_2	1.72
m_1	0.78
k_f	0.69
d_2	0.19
m_f	0.07
d_1	0.02
d_f	0.01

Table 7-7: Model and Model Error Sensitivity Characteristics

Characteristic	Average Model Sensitivity Coefficient	Average Model Error Sensitivity Coefficient
ω	26.39	36.88
ke_1	7.62	8.9
m_2	7.17	8.18
ke_2	3.79	5.23
kp_1	3.48	3.96
Fe	2.12	2.12
m_d	1.76	4.14
kp_2	1.72	2.28
m_1	0.78	0.47
k_f	0.69	1.1
d_2	0.19	0.11
m_f	0.07	0.11
d_1	0.02	0.02
d_f	0.01	0.07

Table 7-8: Rank Order of Model and Model Error Sensitivity Coefficients

Characteristic	Model Sensitivity Coefficient Rank	Model Error Sensitivity Coefficient Rank
ω	1	1
ke_1	2	2
m_2	3	3
ke_2	4	4
kp_1	5	6
Fe	6	8
m_d	7	5
kp_2	8	7
m_1	9	10
k_f	10	9
d_2	11	12
m_f	12	11
d_1	13	14
d_f	14	13

COMPARING SENSITIVITY COEFFICIENTS

The model sensitivity analysis was based on the changes between the calculated values of roller drum deflection for consistent changes in the input characteristics. The model error sensitivity analysis was based on the difference between the calculated and measured values of roller drum deflection. An error in the measured value of roller drum deflection at 1 or more of the test points could affect the magnitude and order of the sensitivity coefficients in the model error sensitivity analysis. The model sensitivity analysis did not rely on a measured value and would not be affected by an error in the measured value. As such, the model sensitivity characteristics are probably more representative of how the model would react to changes in the input characteristics.

MINIMIZING THE DIFFERENCES

The purpose of the error minimization procedure was to determine what values of the soil related input characteristics were required to obtain agreement between the calculated and measured values of roller drum deflection. If realistic values of the input characteristics were obtained it would tend to suggest that the model contained the appropriate input characteristics. Unrealistic values would suggest that unnecessary characteristics were included in the model and/or that important characteristics had been omitted.

Method Used to Minimize Differences

Microsoft Excel contains a solver function which allows for 1 or more input characteristics within an equation to be varied so that the output of the equation will converge to a desired result. The desired result of this study was that the calculated value of roller drum displacement match the measured value of roller drum displacement to within (±) 1%. A 1% error was deemed acceptable because the percent error between field and lab measurements of material density reported in the literature often exceeds 1% (Padlo et al., 2005). The values of the input characteristics were constrained to be equal to, or greater than, 100 to prevent negative values, which have no physical meaning in the model, from being generated.

According to the Microsoft's online help site, the solver function uses the Generalized Reduced Gradient method to solve nonlinear problems. Linear and integer problems are solved by the simplex method and the branch-and-bound method (Microsoft, 2010). Given that the subject model contained terms with both real and imaginary exponents, it is most certainly a nonlinear problem.

Gradients are changes in slope between numbers, which can be thought of in this case as an input characteristic and the solution to the model. At one extreme, gradient slopes can be very steep and approach vertical, which means that a small change in the input characteristic leads to a large change in the output (i.e. a sensitive characteristic). At the other extreme the gradient may be shallow and approach horizontal, which means

that a large change in the input characteristic produces little change in the output (i.e. a non-sensitive characteristic). A gradient change solution method makes small changes in the specified input characteristic or characteristics and then monitors how the changes affect the desired outcome and continues to adjust the characteristics in an efficient way to reach the desired outcome (Revelle et al., 2004).

Just because a solver tool adjusts a series of numbers to achieve the desired outcome does not necessarily mean that the adjusted numbers are correct, or even realistic. The gradient change solution method can be compared to a hiker, without a topographical map of the area, attempting to find the lowest elevation within a series of valleys by simply walking around until it is not possible to go any lower. While the hiker may have found the local minimum within one valley, there is no guarantee that the lowest point within the series of valleys was found. The same holds true for the minimization of the differences between the measured and calculated values of roller drum displacement.

Approach to Difference Minimization

The subject model used to calculate roller drum deflection contains 14 input characteristics. Six of the characteristics describe the roller and 8 characteristics are used to describe the 2 soil layers. The values that describe the roller were considered to be fixed because they were either known with a reasonable degree of certainty, or do not appreciably change with the degree of compaction or variations in soil layer depth and mass. As such, the minimization procedures focused exclusively on varying some or all of the 8 soil related characteristics at each point.

Results of Difference Minimizations

Adjustment of all 8 Soil Related Characteristics

The solver tool tended to focus on making large adjustments to the mass when the initial values of all 8 soil related characteristics were allowed to vary. Point 5 did not follow this general trend in that the damping characteristics were increased by about 300 to 400% in order to reach 1% agreement. The results of the error minimization for each test point are shown in Table 7-9.

Allowing all 8 soil related characteristics to vary in the error minimization did not appear to be valid for several reasons. First, the final masses at Point 5 both decreased to the limiting value of 100 kg (220.5 lbs) to reach closure. These values are both unreasonable and probably explain why the values of the damping characteristics increased by such high percentages. Second, the minimization tended to focus on the mass of the first and second soil layers to reach closure. This is not surprising given the fact that the model is highly sensitive to the mass of the second soil layer. Third, the soil damping is related to the elastic stiffness, which was not adjusted during the minimization.

Table 7-9: Percent Change in Initial Input Values When All Eight Soil Related Characteristics Were Allowed to be Adjusted

Point	m_1	m_2	kp_1	kp_2	ke_1	ke_2	d_1	d_2
1	-9.05	-37.64	0.00	0.00	0.00	0.00	0.00	0.00
2	2.06	3.61	0.00	0.00	0.00	0.00	0.00	0.00
3	-3.23	-24.88	0.00	0.00	0.00	0.00	0.00	0.00
4	-1.45	-24.28	0.00	0.00	0.00	0.00	0.00	0.00
5	-93.13	-88.72	0.00	0.00	0.00	0.00	291.46	416.56
6	336.05	79.43	0.00	0.00	0.00	0.00	0.00	0.00

Adjustment of Only the Soil Masses

The results of the error minimization when only the masses were allowed to be varied were similar to the results of 8 soil characteristic minimization, as shown in Table 7-10. Specifically, the masses of Layer 1 and Layer 2 at Point 5 were reduced to the minimum value of 100 kg (220.5 lbs), which was unrealistic. The large increase in the Layer 1 mass at Point 6 were also unrealistic given that the change in Layer 1 mass at Points 1 through 4 was relatively minor.

Table 7-10: Percent Change in Initial Input Values When the Soil Masses Were Allowed to be Adjusted

Point	m_1	m_2	kp_1	kp_2	ke_1	ke_2	d_1	d_2
1	-6.52	-37.72	0.00	0.00	0.00	0.00	-3.31	-21.08
2	2.25	3.93	0.00	0.00	0.00	0.00	1.12	1.94
3	-3.16	-24.56	0.00	0.00	0.00	0.00	-1.59	-13.14
4	-0.92	-23.98	0.00	0.00	0.00	0.00	-0.46	-12.81
5	-93.13	-88.72	0.00	0.00	0.00	0.00	-73.79	-66.41
6	358.13	79.66	0.00	0.00	0.00	0.00	114.04	34.04

Adjustment of Soil Elastic Stiffness Characteristics

The soil elastic stiffness characteristics (ke_1 and ke_2) were allowed to vary so that their effect on the calculated value of roller drum deflection could be observed. As previously stated, the values of the plastic stiffness and damping characteristics depend upon the value of the corresponding elastic stiffness characteristic. The path the solver tool used to minimize the difference between the calculated and measured values of roller drum deflection depended upon the initial difference between the 2 deflections. The layer 1 elastic stiffness characteristics were increased from their initial values if the initial difference between the drum deflections was positive (i.e. the calculated value of roller drum deflection was greater than the measured value of roller drum deflection).

The layer 1 elastic stiffness characteristics were decreased if the initial difference between the two deflections was negative. Table 7-11 contains a summary of the percent change in stiffness and damping characteristic values needed to obtain a closure between the measured and calculated roller drum deflections of approximately 1%.

Table 7-11: Percent Change in Stiffness and Damping Characteristics When Elastic Stiffness Characteristics Were Adjusted

Point	kp_1	kp_2	ke_1	ke_2	d_1	d_2
1	10.74	64.25	10.74	64.25	5.23	28.16
2	-33.83	45.92	-33.83	45.92	-18.66	20.80
3	19.51	18.75	19.51	18.75	9.32	8.97
4	27.07	16.13	27.07	16.13	12.72	7.76
5	-39.42	-7.41	-39.42	-7.41	-22.17	-3.78
6	-70.93	105.27	-70.93	105.27	-46.09	43.27

The formulas for the plastic stiffness and damping characteristics used in the Excel spreadsheet depend upon the elastic stiffness characteristic within each layer. For example, the plastic stiffness characteristic was set to be 87% of the layer's elastic stiffness characteristic (Pietzsch and Poppy, 1992). As such, raising and lowering the values of the elastic stiffness characteristics caused the values of the plastic stiffness and damping characteristics to change as well. This phenomenon is illustrated by the fact that the percent change in the elastic and plastic stiffness characteristics were equal and that the percent change in the damping characteristics were essentially one-half the percent change in the elastic characteristics.

The final values of the elastic and plastic stiffness characteristics were converted into elastic moduli to determine if the final values of these characteristics were realistic. The conversion was accomplished by reversing the procedure that was used to find the initial values of the elastic stiffness characteristics using the soil layer modulus values obtained by pFWD tests. The plastic stiffness characteristics were treated as elastic

stiffnesses because the literature contained very little information on plastic moduli related to soil. The results of the conversion are displayed in Table 7-12.

Table 7-12: Final Moduli When only Elastic Stiffness Was Varied

Point	Ep_1 (GPa)	Ep_2 (GPa)	Ee_1 (GPa)	Ee_1(psi)	Ee_2 (GPa)	Ee_2 (psi)
1	0.066	0.067	0.076	11,023	0.077	11,168
2	0.052	0.078	0.060	8,702	0.090	13,053
3	0.057	0.054	0.065	9,427	0.062	8,992
4	0.072	0.070	0.083	12,038	0.081	11,748
5	0.042	0.069	0.048	6,962	0.079	11,458
6	0.050	0.164	0.057	8,267	0.189	27,412

The literature reported that an unspecified rubber material, which was subjected to small strains, had an elastic stiffness on the order of 0.01 to 0.1 GPa (1,500 to 15,000 psi) (Engineer's Toolbox, 2010). The majority of the final modulus values fell within the middle of the given range, with the elastic and plastic moduli of Test Point 6's first layer exceeding the range. These results appear to be reasonable given that the tested material was a hard clay soil undergoing small strains because the specified degree of compaction had reportedly been achieved. As a point of comparison, the Young's modulus for 29,000 ksi steel is 200 GPa.

The initial values of the elastic stiffnesses used in the model were based on average values of elastic moduli obtained from pFWD tests. Resilient modulus tests were also conducted on several soil samples from the site. A comparison of the starting and ending values of elastic moduli with the moduli obtained from pFWD and resilient modulus testing is contained in Table 7-13. The table shows that almost all of the final values of the elastic moduli needed to obtain a closure of 1% between the calculated and measured amount of roller drum deflection fell within the range of the values obtained in the field and the laboratory.

Table 7-13: Initial and Final Model Moduli Compared to Field and Lab Tests

Point	Layer	Initial Input Value of Elastic Modulus (psi)	Final Value of Elastic Modulus (psi)	pFWD Moduli (psi) [values from all three sensors]	Lab Resilient Moduli (psi)
1	1	6,768	11,023	5,656 to 12,328	7,000 to 14,000
1	2	9,910	11,168		
2	1	8,919	8,702	4,786 to 16,824	No Tests Conducted
2	2	13,101	13,053		
3	1	7,614	9,427	5,221 to 10,588	8,000 to 19,000
3	2	7,928	8,992		
4	1	10,079	12,038	6,962 to 12,328	6,000 to 18,000
4	2	9,499	11,748		
5	1	12,400	6,962	11,458 to 12,618	10,000 to 22,000
5	2	11,457	11,458		
6	1	13,342	8,267	13,198 to 28,717	47,000 to 91,000
6	2	28,425	27,415		

The fact that the overwhelming majority of the final moduli values fell within the ranges of the field and laboratory moduli was a further indication that the model can accurately predict the degree of compaction of the upper soil layer. The discrepancies between the starting and ending moduli values were probably caused by a couple of factors. First, the pFWD cannot isolate the first soil layer from the second soil layer. As such, the modulus value calculated for sensor 1 depends upon the soil throughout the entire test depth. The third sensor is affected by the lower soil, but there is no guarantee that the soil lies only within the second soil layer used in the model. Second, it is quite possible that the samples used in the resilient modulus testing contained soil from both the top and bottom soil layers.

CHAPTER VIII
CONCLUSION

SUMMARY

This project focused on the development of a mechanics based soil-roller interaction model capable of determining the degree of compaction of the top layer of a soil profile. The model was an extension of work performed by others who sought to determine the effects of theoretical modifications to vibratory rollers without the need to build working prototypes (Pietzsch and Poppy, 1992; Yoo and Selig, 1972). This model included 2 non-uniform soil layers instead of treating the soil as a single, homogeneous mass as many previous models have. The multilayer approach has the potential to more accurately capture the conditions encountered on actual construction projects.

An accelerometer based monitoring system was attached to a vibratory smooth drum roller in an attempt to determine the degree of compaction of the top soil layer. The roller was then driven across a number of test sections and the displacement of the roller drum was determined from the measured acceleration of the roller drum. The test sections included portions of active construction projects such as roadways and running tracks, as well as in-service gravel roads and parking lots. Baseline testing of the soil within the test sections was conducted before and after the roller was driven across the test sections. The baseline tests included; dry and wet density by nuclear methods, DCP penetration rate, pFWD and FWD back calculated moduli and wet and dry density determined by laboratory testing of Shelby tube samples.

FINDINGS

A sum-of-the-square of the errors (best fit line) procedure was used to determine if a causal relationship existed between the gathered baseline soil data, roller drum deflection and the degree of compaction of the upper soil layer. Analysis of the data revealed that there was no evident correlation between roller drum deflection and the degree of compaction of the upper soil layer when roller drum deflection was compared

to only 1 of the input characteristics. The lack of correlation was not surprising given the number of characteristics that contribute to soil compaction and the measured deflection of the roller drum.

The accuracy of the mechanics based soil-roller-interaction-model was tested against the results of baseline measurements and data obtained from two SH 21 test sections. The model should be considered to be accurate if the calculated value of roller drum deflection was within 1% of the measured value of roller drum deflection. Additional model parameters/inputs such as elastic and plastic spring stiffness, damping values, eccentric mass frequency and roller drum force were obtained from manufacturer's literature and research by others (Caterpillar, 2003; Pietz and Poppy, 1992; Rinehart and Mooney, 2005; Richart et al., 1970). The difference between the calculated values of roller drum deflection and the measured values of roller drum deflection using the initial estimated values of the input characteristics ranged from approximately -95% to 935%.

An error minimization procedure using the solver tool in Microsoft Excel (2010) was used to adjust several of the soil related characteristics in an attempt to decrease the error between the calculated and measured values of roller drum deflection to approximately 1%. The minimization process suggested that the model could accurately predict the degree of compaction of the upper soil layer. The moduli that were back calculated from the final stiffnesses needed to reach a 1% closure generally fell within the range of the moduli resulting from pFWD and resilient modulus testing. Had the error minimization process resulted in excessively high or low back calculated moduli it would probably have been necessary to adjust the input characteristics.

Both the model error sensitivity analysis and the model sensitivity analysis showed that the mass of the second soil layer was an important characteristic. In fact, the model was, on average, 9 to 17 times more sensitive to changes in the mass of the second layer than it was to changes in the mass of the first layer. This result suggests that any model attempting to determine the degree of compaction must be composed of at least 2 layers. The importance of the mass of the second soil layer, m_2, is probably

caused by the fact that the second soil layer acts as the anvil upon which the top layer is compacted. A poorly compacted, or soft, underlying layer makes it difficult to compact the top layer (Holtz and Kovacs, 1981).

The sensitivity analysis also showed that the model was more sensitive to changes in the elastic and plastic stiffnesses than to the mass of the top soil layer. This is an important finding in that the low sensitivity of the mass of the top soil layer, and by extension the density of the top soil layer, means that large changes in the mass of layer 1 would have minimal effects on the output of the model. This characteristic is a drawback if the fill is to be installed and tested according to standard density specifications. However, this characteristic would be an advantage if the fill is to be installed and tested according to a specification based on the design material modulus or stiffness.

As previously stated, roadways are not designed on the basis of the density of their component parts; they are designed based on stiffness or modulus. The fact that most specifications use a density based acceptance criteria is probably based more on convenience and the availability of equipment that can accurately determine density in the field. Fortunately, equipment that can accurately determine the modulus or stiffness of a material in the field is becoming available and governing agencies are beginning to develop specifications to address these advances.

RECOMMENDATIONS

Future measuring systems should contain at least 2 accelerometers so that the redundancy in the model may be used to minimize the errors. Additionally, the installation of a second pair of accelerometers on the roller frame could improve the accuracy of the model by allowing the equation for the displacement of the roller frame to be evaluated. The second set of accelerometers would also provide a way to accurately determine the stiffness and damping of the roller frame (k_f and d_f).

The plastic spring characteristics were set as a percentage of the elastic spring characteristics in the Excel spreadsheet. A more correct procedure may involve

developing an equation along the line of what was used to determine the initial values of the elastic spring characteristics from the pFWD data so that the elastic an plastic spring values are uncoupled from each other. Such a procedure would probably entail laboratory testing of soil samples to determine the relationship between a compacted soil sample subjected to elastic and plastic deformations.

Additional testing is required to determine how best to model the roller drum vibration distribution pattern, which has a direct impact on the mass of the first and second soil layers. The current model used a triangular distribution pattern whose lateral spread was limited by the outside edges of the roller drum. Other distribution patterns could be steeper or shallower, and/or extend beyond the outside edges of the roller drum. Implanting accelerometers into the soil mass could provide insight to the correct distribution pattern and may also allow for more rigorous testing of the model by providing the information needed to test the equations describing the displacement of the two soil layers.

REFERENCES

American Society for Testing Materials (ASTM), 2001. Annual Book of ASTM Standards, Section 4, Construction, 04.08 Soil and Rock (I): D420-D5779. ASTM, West Conshohocken, PA.

Anderegg, R., Kaufmann, K., 2004. Intelligent compaction with vibratory rollers – feedback control systems in automatic compaction and compaction control. Transportation Research Record 1868, TRB, National Research Council, Washington, DC, pp.124-134.

Assouline, S., 2002. Modeling soil compaction under uniaxial compression. Soil Science Society of America Journal. 66, 1784-1787.

Bardet, J.P., 1997. Experimental Soil Mechanics. Prentice Hall, Upper Saddle River, NJ.

Brock, D.S., Sutcliffe, Jr., L.L., 1986. Field Inspection Handbook, An On-The-Job Guide for Construction Inspectors, Contractors, Architects, & Engineers. McGraw-Hill, New York, NY.

Canillas, E.C., 2001. Regression analysis of some factors influencing soil compaction. Soil & Tillage Research. 61, 167-178.

Caterpillar Incorporated, 2003. Caterpillar Performance Handbook, thirty-forth ed. Caterpillar Incorporated, Peoria, IL.

Das, B.M., 1999. Principles of Foundation Engineering, forth ed. PWS Publishing, Albany, NY.

Dunham, C.W., 1962. Foundations of Structures, second ed. McGraw-Hill, New York, NY.

Engineer's Toolbox. Young's Modulus. http://www.engineeringtoolbox.com/young-modulus-d_417.html. Accessed July 20, 2010.

Fredlund, D.G., Rahardjo, H., 1993. Soil Mechanics for Unsaturated Soils. Wiley Inter-Science, New York, NY.

Ghezzehei, T.A., Or, D., 2001. Rheological properties of wet soils and clays under steady and oscillatory stresses. Soil Science Society of America Journal. 65, 624-637.

Grift, T.E., Tekeste, M.Z., Raper, R.L., 2005. Acoustic compaction layer detection. Transactions of the American Society of Agricultural and Biological Engineers. 48(5), 1723-1730.

Haas, R., Hudson, W.R., Zaniewski, J., 1994. Modern Pavement Management. Krieger Publishing Company, Malabar, FL.

Holtz, R.D., Kovacs, W.D., 1981. An Introduction to Geotechnical Engineering. Prentice Hall, Englewood Cliffs, NJ.

Huang, Y.H., 2004. Pavement Analysis and Design, second ed. Pearson Prentice-Hall, Upper Saddle River, NJ.

Jonsson, A., Bathelt, J., Broman, G., 2004. Implications of modeling one-dimensional impact by using a spring and damper element. In: Proceedings of the Institute of Mechanical Engineering (IMechE). 219, Part K, 299-305.

Kessler Soils Engineering Products, Inc., 2005. Kessler DCP Dynamic Cone Penetrometer Model 100 User's Manual. Kessler Soils Engineering Products, Inc., Springfield, VA.

Liu, C., Evett, J.B., 2008. Soils and Foundations, seventh ed. Pearson-Prentice Hall, Upper Saddle River, NJ.

Lytton, R.L., 1989. Back calculation of pavement layer properties. In: Bush III, A.J. (Ed.), Nondestructive Testing of Pavements and Back Calculation of Moduli, ASTM STP 1026, American Society for Testing and Materials, Philadelphia, PA, 7-38.

McCarthy, D.F., 2007. Essentials of Soil Mechanics and Foundations, seventh ed. Prentice Hall, Upper Saddle River, NJ.

Microsoft. Help and How-to: About Solver. http://office.microsoft.com/assistance. Accessed April 9, 2010.

Mitchell, J.K., Soga, K., 2005. Fundamentals of Soil Behavior, third ed. John Wiley & Sons, Inc., Hoboken, NJ.

Or, D., Ghezzehei, T.A., 2002. Modeling post-tillage soil structure dynamics: a review. Soil and Tillage Research. 64, 41-59.

Padlo, P.T., Mahoney, J., Aultman, L., Zinke, S., 2005. Correlation of Nuclear Density Readings with Cores Cut from Compacted Roadways. Report CT-2242-F-05-5. Connecticut Transportation Institute, University of Connecticut, Storrs, CT.

Peterson, D.L., Erickson, M., Roberson, R., Siekmeier, J., 2007. In TRB 2007 Annual Meeting CD-ROM, Transportation Research Board, National Research Council, Washington, DC.

Pietzsch, D., Poppy, W., 1992. Simulation of soil compaction with vibratory rollers. Journal of Terramechanics. 29, No. 6, 585-597.

Rahman, F., Hossain, M., Hunt, M., Romanoschi. S., 2007. In TRB 2007 Annual Meeting CD-ROM, Transportation Research Board, National Research Council, Washington DC.

Revelle, C.S., Whitlatch, E.E., Wright, J.R., 2004. Civil and Environmental Systems Engineering, second ed. Prentice-Hall, Upper Saddle River, NJ.

Richart, F.E., Hall, J.R., Woods, R.D., 1970. Vibrations of Soils and Foundations. Prentice-Hall, Englewood Cliffs, NJ.

Rinehart, R.V., Mooney, M.A., 2005. Instrumentation of a roller compactor to monitor vibration behavior during earthwork compaction. In: Twenty-second International Symposium on Automation and Robotics in Construction. Ferrara, Italy, pp. 1-6.

Rinehart, R.V., Mooney, M.A., 2009. Measurement depth of vibratory roller-measured soil stiffness. Geotechnique. 59, No. 7, 609-619.

Saeys, W., Mouazen, A.M., Anthonis, J., Ramon, H., 2004. An automatic depth control system for online measurement of spatial variation in soil compaction, part 2: modeling of the depth control system. Biosystems Engineering. 89, No. 3, 267-280.

Scheaffer, R.L., McClave, J.T., 1990. Probability and Statistics for Engineers. third ed. PWS-Kent, Boston, MA.

Scullion, T., Sebesta, S., Rich, D., Liu, W., 2006. Field Evaluation of New Technologies for Measuring Pavement Quality. Report 0-4774-2. Texas Transportation Institute, Texas A&M University System, College Station, TX.

Scullion, T., Briggs, R. C., Lytton, R.L., 1989. Using the Multidepth Deflectometer to Verify Modulus Back Calculation Procedures. Nondestructive Testing of Pavements and Back Calculation of Moduli, ASTM STP 1026, A. J. Bush III and G. Y. Baladi, Eds., American Society for Testing and Materials, Philadelphia, PA, 90-101.

Sears, F.W., Zemansky, M.W., Young, H.D., 1987. University Physics, seventh ed. Addison-Wesley, Reading, MA.

Spangler, M.G., Handy, R.L., 1982. Soil Engineering, fourth ed. Harper and Row, New York, NY.

StatPac Inc. Correlation Types. http://www.statpac.com/ statistics-calculator/correlation-regression.htm. Accessed January 4, 2010.

Tateyama, K., Ashida, S., Fukagawa, R., Takahashi, H., 2006. Geomechatronics-interaction between ground and construction machinery and its application to construction robotics. Journal of Terramechanics. 43, 341-353.

Texas Department of Transportation. Guide Schedule for Sampling and Testing. Austin, TX, April 2005. http://www.dot.state.tx.us/pub/txdot-info/cmd/guide_ schedule.pdf. Accessed May 8, 2007.

Thurner, H.F., Sandstrom, A. Continuous Compaction Control, CCC. In: European Workshop Compaction of Soils and Granular Materials. Paris, France, May 19th 2000, pp. 237-246.

Troxler Electronic Laboratories Inc. Road Reader Nuclear Density Gauges. http://troxlerlabs.com. Research Triangle Park, NC, 2009. Accessed April 21, 2010.

Way, T.R., Erbach, D.C., Bailey, A.C., Burt, E.C., Johnson, C.E., 2005. Soil displacement beneath an agricultural tractor drive tire. Journal of Terramechanics. 42, No. 1, 35-46.

Wolf, J.P., 1994. Foundation Vibration Analysis Using Simple Physical Models. Prentice Hall, Upper Saddle River, NJ.

Wolf, J.P., and Deeks, A.J., 2004. Foundation Vibration Analysis: A Strength-of-materials Approach. Elsevier, Burlington, VT.

Yoder, E.J., Witczak, M.W., 1975. Principles of Pavement Design, second ed. John Wiley & Sons, New York, NY.

Yoo, T.S., Selig, E.T., 1979. Dynamics of vibratory-roller compaction. Journal of the Geotechnical Engineering Division. ASCE. 105, No. 10, 1211-1231.

APPENDIX A

MISCELLANEOUS FIGURES

TYPICAL FREQUENCY DISTRIBUTION PLOT

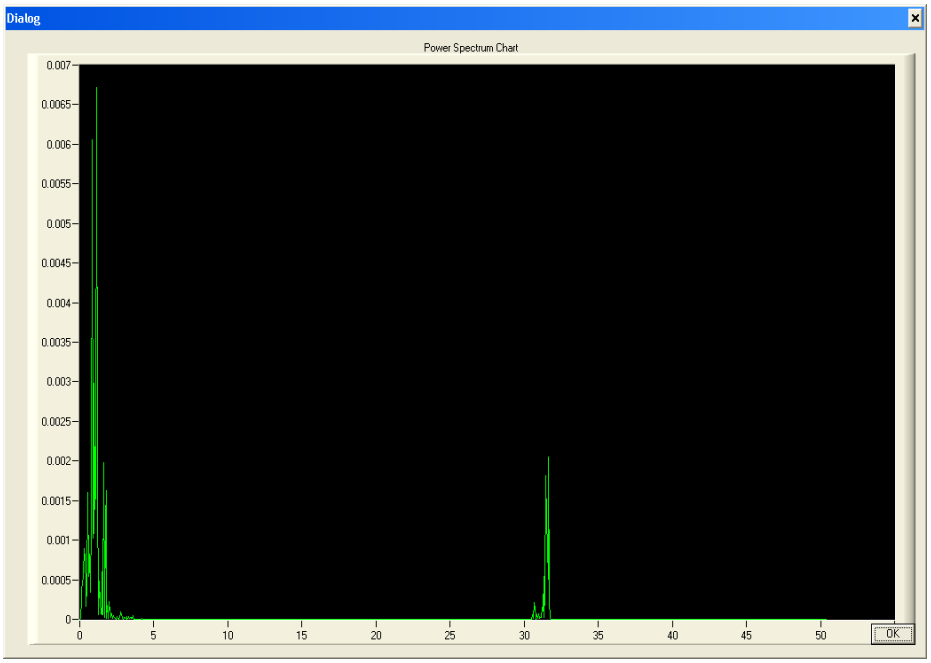

Fig. A-1. Frequency distribution plot showing roller drum displacements along the Y-axis as a function of the frequency at which the displacements occur along the X-axis.

TYPICAL RAMS OUTPUT

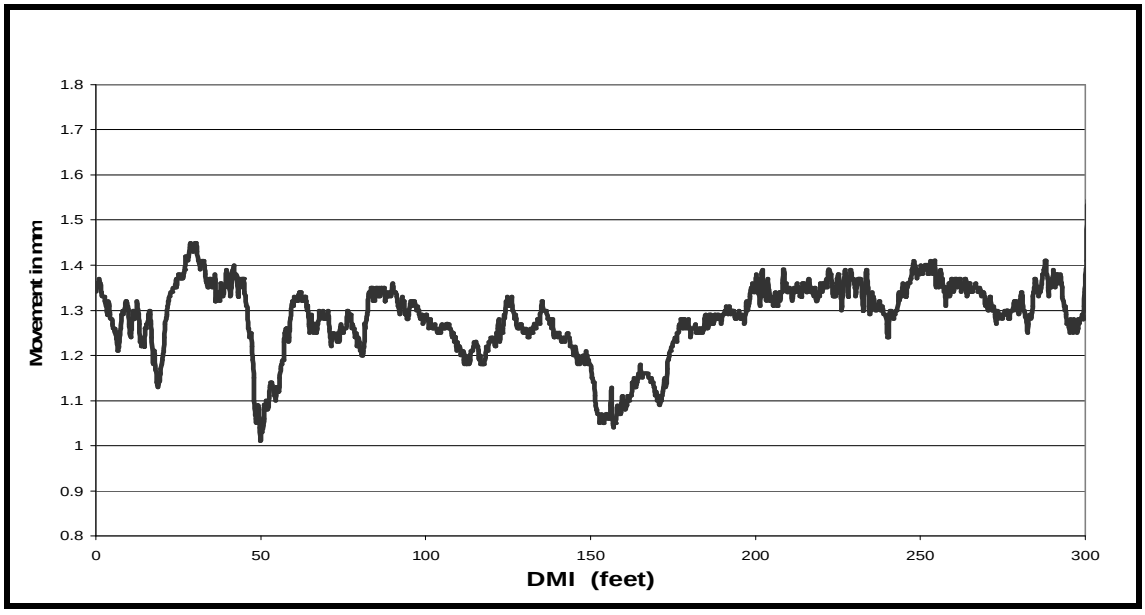

Fig. A-2. Roller drum displacements versus distance along test strip. Figure courtesy of Dr. Wenting Liu.

APPENDIX B
DERIVATION OF THE MODEL

SCHEMATIC AND MODEL CHARACTERISTICS

This portion of the Appendix presents a detailed derivation of the soil-roller interaction model, which was generally described in Chapter VI. Figure A-3 illustrates the components of the model while Table A-1 defines the characteristics and units for each characteristic within the model.

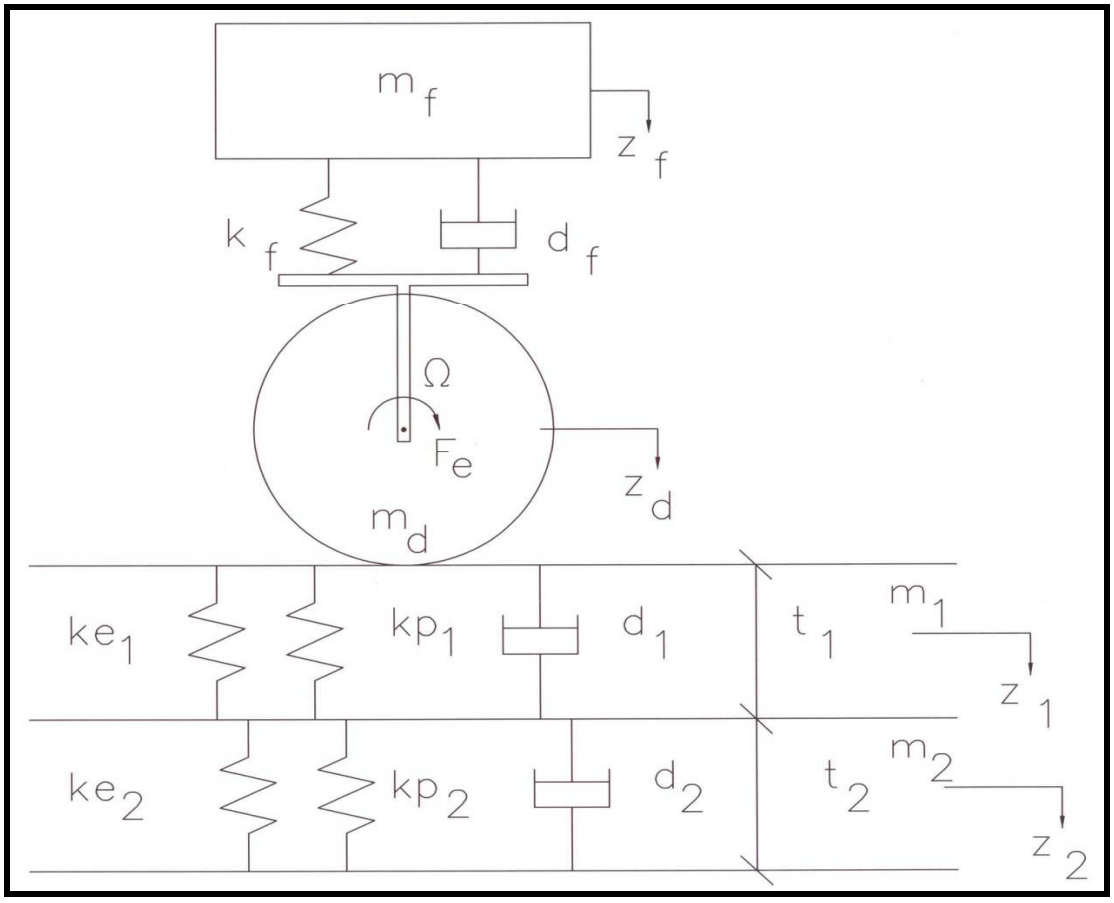

Fig. B-1. Schematic of the model components.

The “T” shaped bar that connects the roller frame to the roller drum is a massless construct that is used to show that the frame stiffness and damping connect to the roller drum at the drum axle.

Table B-1: Model Characteristics and Units

Symbol	**Description**	**Units**
m_f	mass of drum frame	mass
z_f	displacement of drum frame	length
k_f	elastic stiffness between drum frame and drum	force/length
d_f	damping between drum frame and drum	force*time/length
F_e	exciting force	force
Ω or ω	frequency of eccentric mass	Hertz
m_d	mass of drum	mass
z_d	displacement of drum	length
k_{e1}	elastic stiffness of top soil layer	force/length
k_{p1}	plastic stiffness of top soil layer	force/length
t_1	thickness of top soil layer	length
d_1	damping of top soil layer	force*time/length
m_1	mass of the first soil layer	mass
z_1	displacement of top soil layer	length
k_{e2}	elastic stiffness of lower soil layer	force/length
k_{p2}	plastic stiffness of lower soil layer	force/length
t_2	thickness of lower soil layer	length
d_2	damping of lower soil layer	force*time/length
m_2	mass of the second soil layer	mass
z_2	displacement of lower soil layer	length

FREE BODY DIAGRAMS

The free body diagrams of each of the four model components were constructed and used to develop the model equations. The free body diagrams and base equations for each component are shown below.

Roller Frame

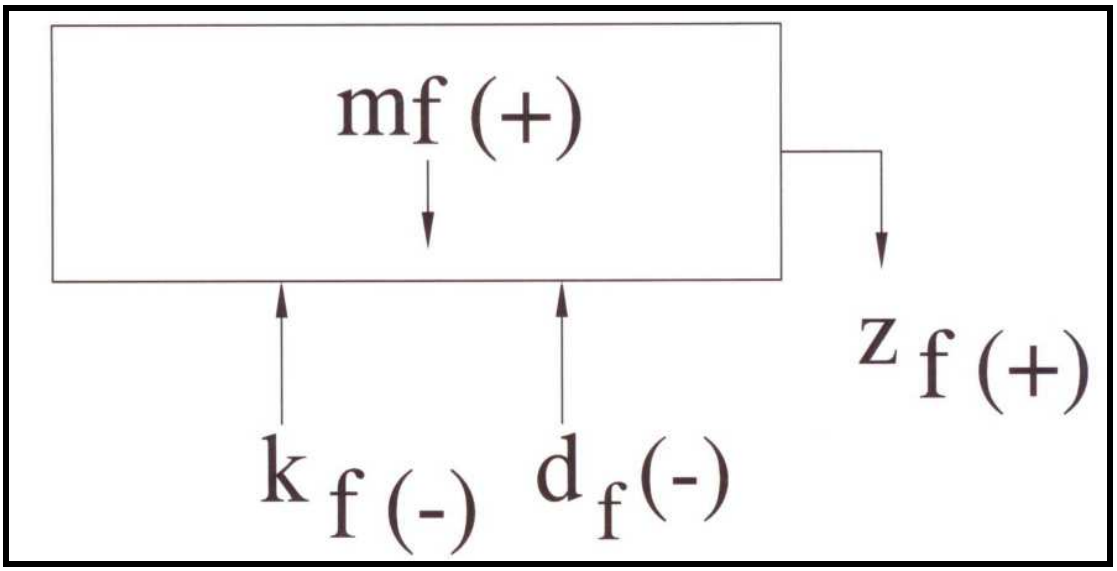

Fig. B-2. Free body diagram of roller frame.

Model equation for roller frame (base equation 1):

$m_f (z''_f) = - k_f(z_f-z_d)-d_f(z'_f-z'_d)$

Roller Drum

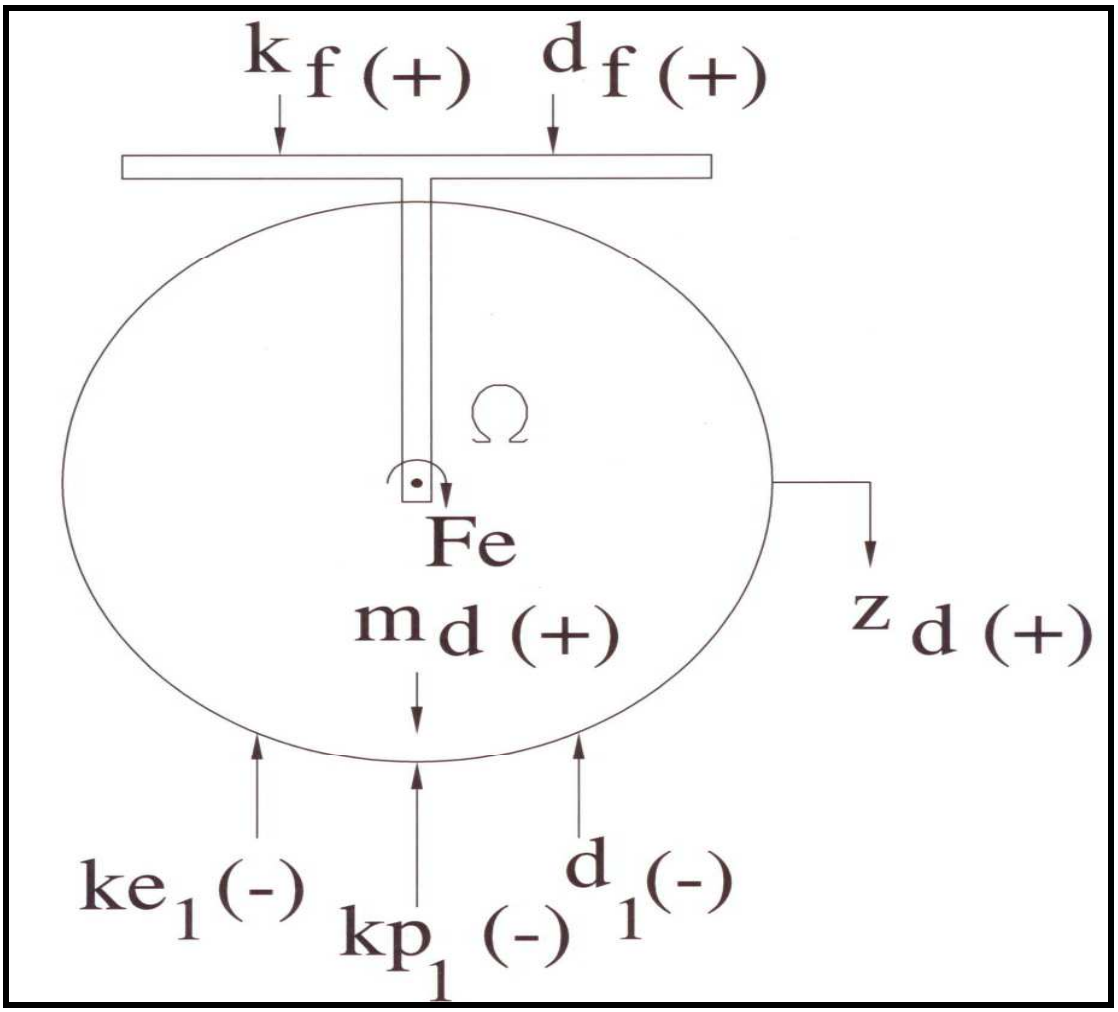

Fig. B-3. Free body diagram of roller drum.

Model equation for roller drum (base equation 2):

$m_d(z''_d)- F_e = k_f (z_f-z_d)+d_f(z'_f-z'_d)-k_{e1}(z_d-z_1)-k_{p1}(z_d-z_1)-d_1(z'_d-z'_1)$

Soil Layer 1

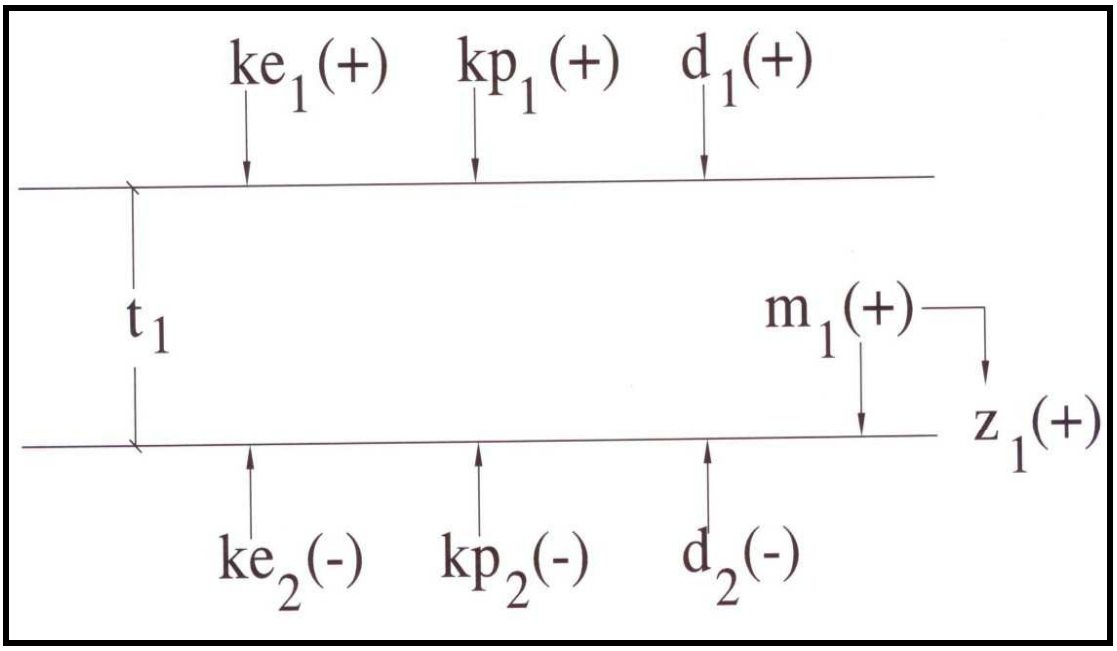

Fig. B-4. Free body diagram of soil layer 1.

Model equation for soil layer 1 (base equation 3):

$m_1(z''_1)= k_{e1}(z_d-z_1)+k_{p1}(z_d-z_1)+ d_1(z'_d-z'_1)- k_{e2}(z_1-z_2)-k_{p2}(z_1-z_2)- d_1(z'_1-z'_2)$

Soil Layer 2

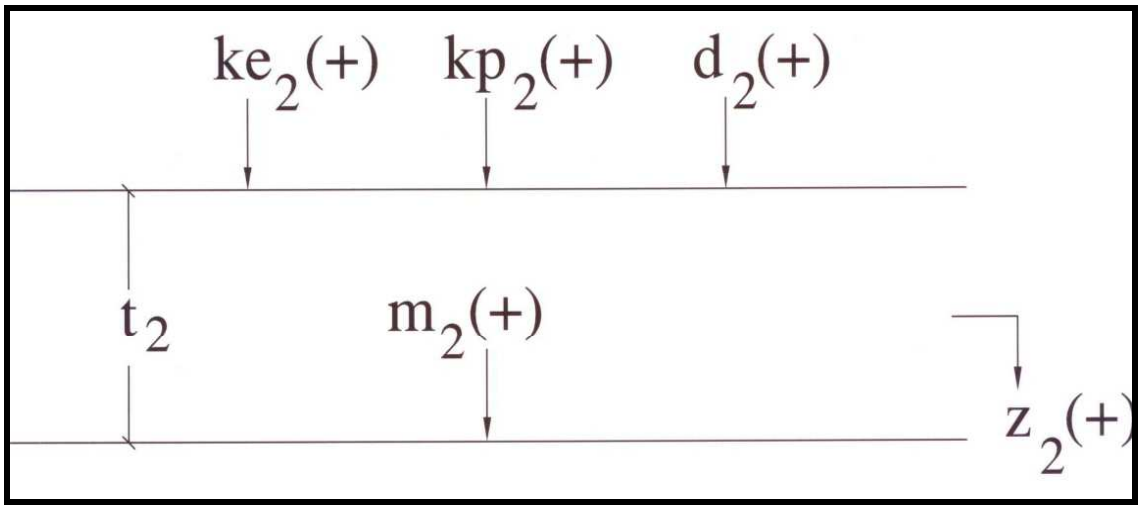

Fig. B-5. Free body diagram of soil layer 1.

Free body diagram equation for soil layer 2 (base equation 4):

$m_2(z''_2)= k_{e2}(z_1-z_2)+ k_{p2}(z_1-z_2)+ d_2(z'_1-z'_2)$

EFFECTS OF DAMPING

The amount of force imparted to the roller frame and soil layers by the roller drum varies with the position of the rotating eccentric mass within the roller drum. The damping between the drum and the frame, and the damping within each soil layer, causes the force to be felt at a slightly later time than the load is imparted (Richart et al 1970). This means that the maximum displacements, velocities and accelerations within each component lag behind the forcing function provided by the roller drum. As such, the characteristics representing displacement, velocity and acceleration must be

expanded into the following equations or identities to account for the lag effect (Pietzsch and Poppy 1992; Richart et al 1970; Yoo and Selig 1979).

Roller Frame

$z_f = Z_f e^{-i(\omega t-\Phi f)}$

$z'_f = -i\omega\, Z_f e^{-i(\omega t-\Phi f)}$

$z''_f = -\omega^2 Z_f e^{-i(\omega t-\Phi f)}$

Roller Drum

$z_d = Z_d e^{-i\omega t}$

$z'_d = -i\omega Z_d e^{-i\omega t}$

$z''_d = -\omega^2 Z_d e^{-i\omega t}$

Soil Layer 1

$z_1 = Z_1 e^{-i(\omega t-\Phi 1)}$

$z'_1 = -i\omega Z_1 e^{-i(\omega t-\Phi 1)}$

$z''_1 = -\omega^2 Z_1 e^{-i(\omega t-\Phi 1)}$

Soil Layer 2

$z_2 = Z_2 e^{-i(\omega t-\Phi 2)}$

$z'_2 = -i\omega Z_2 e^{-i(\omega t-\Phi 2)}$

$z''_2 = -\omega^2 Z_2 e^{-i(\omega t-\Phi 2)}$

Where:

Z = the maximum amplitude of the component displacement

$i^2 = -1$

Φf = lag angle of frame

$\Phi 1$ = lag angle of layer 1

$\Phi 2$ = lag angle of layer 2

′ = first derivative of displacement (velocity)

″ = second derivative of displacement (acceleration)

The lag angle represents the degree to which the subject component is out of phase with the forcing function. The identities describing the roller drum do not contain a lag angle because there is no delay because it is the drum that provides the forcing function.

SUBSTITUTION INTO THE FOUR BASE EQUATIONS

The lag identities developed above are substituted into the four base equations as outlined below.

Roller Frame

$$-m_f\omega^2(Z_fe^{-i(\omega t-\Phi f)}) = -k_f(Z_fe^{-i(\omega t-\Phi f)}-Z_de^{-i\omega t})+d_fi\omega(Z_fe^{-i(\omega t-\Phi f)}-Z_de^{-i\omega t})$$

Roller Drum

$$-m_d\omega^2(Z_de^{-i\omega t}) = k_f(Z_fe^{-i(\omega t-\Phi f)}-Z_de^{-i\omega t})-d_fi\omega(Z_fe^{-i(\omega t-\Phi f)}+Z_de^{-i\omega t})-k_{e1}(Z_de^{-i\omega t}-Z_1e^{-i(\omega t-\Phi 1)})$$
$$-k_{p1}(Z_de^{-i\omega t}-Z_1e^{-i(\omega t-\Phi 1)})+i\omega d_1(Z_de^{-i\omega t}-Z_1e^{-i(\omega t-\Phi 1)})+F_e$$

Soil Layer 1

$$-m_1\omega^2(Z_1e^{-i(\omega t-\Phi 1)}) = k_{e1}(Z_de^{-i\omega t}-Z_1e^{-i(\omega t-\Phi 1)})+ k_{p1}(Z_de^{-i\omega t}-Z_1e^{-i(\omega t-\Phi 1)})- i\omega d_1(Z_de^{-i\omega t}-Z_1e^{-i(\omega t-\Phi 1)})$$
$$- k_{e2}(Z_1e^{-i(\omega t-\Phi 1)}-Z_2e^{-i(\omega t-\Phi 2)})-k_{p2}(Z_1e^{-i(\omega t-\Phi 1)}-Z_2e^{-i(\omega t-\Phi 2)})+i\omega d_2(Z_1e^{-i(\omega t-\Phi 1)}-Z_2e^{-i(\omega t-\Phi 2)})$$

Soil Layer 2

$$-m_2\omega^2(Z_2e^{-i(\omega t-\Phi 2)}) = k_{e2}(Z_1e^{-i(\omega t-\Phi 1)}-Z_2e^{-i(\omega t-\Phi 2)})+k_{p2}(Z_1e^{-i(\omega t-\Phi 1)}-Z_2e^{-i(\omega t-\Phi 2)})$$
$$-i\omega d_2(Z_1e^{-i(\omega t-\Phi 1}-Z_2e^{-i(\omega t-\Phi 2)})$$

COMBINE COMPONENT EQUATIONS

Frame and Drum Equation

$$m_f z''_f + m_d z''_d = -m_f\omega^2(Z_f e^{-i(\omega t-\Phi f)}) - m_d\omega^2(Z_d e^{-i\omega t}) + F_e$$

expand, gather terms, and simplify

$$-m_f\omega^2(Z_f e^{-i(\omega t-\Phi f)}) - m_d\omega^2(Z_d e^{-i\omega t}) = k_{e1}(Z_d e^{-i\omega t} - Z_1 e^{-i(\omega t-\Phi 1)}) - k_{p1}(Z_d e^{-i\omega t} - Z_1 e^{-i(\omega t-\Phi 1)}) + i\omega d_1(Z_d e^{-i\omega t} - Z_1 e^{-i(\omega t-\Phi 1)}) + F_e$$

Frame, Drum, and Layer 1 Equation

$$m_f z''_f + m_d z''_d + m_1 z''_1 = -m_f\omega^2(Z_f e^{-i(\omega t-\Phi f)}) - m_d\omega^2(Z_d e^{-i\omega t}) - m_1\omega^2(Z_1 e^{-i(\omega t-\Phi 1)})$$

expand, gather terms, and simplify

$$-m_f\omega^2(Z_f e^{-i(\omega t-\Phi f)}) - m_d\omega^2(Z_d e^{-i\omega t}) - m_1\omega^2(Z_1 e^{-i(\omega t-\Phi 1)}) = -k_{e2}(Z_1 e^{-i(\omega t-\Phi 1)} - Z_2 e^{-i(\omega t-\Phi 2)}) - k_{p2}(Z_1 e^{-i(\omega t-\Phi 1)} - Z_2 e^{-i(\omega t-\Phi 2)}) + i\omega d_2(Z_1 e^{-i(\omega t-\Phi 1)} - Z_2 e^{-i(\omega t-\Phi 2)}) + F_e$$

Frame, Drum, Layer 1, and Layer 2 Equation

$$m_f\omega^2(Z_f e^{-i(\omega t-\Phi f)}) + m_d\omega^2(Z_d e^{-i\omega t}) + m_1\omega^2(Z_1 e^{-i(\omega t-\Phi 1)}) + m_2\omega^2(Z_2 e^{-i(\omega t-\Phi 2)}) = F_e$$

Let:

$Z_f e^{-i(\omega t-\Phi f)} = X1$ = displacement of the frame

$Z_d e^{-i\omega t} = X2$ = displacement of the drum

$Z_1 e^{-i(\omega t-\Phi 1)} = X3$ = displacement of soil layer 1

$Z_2 e^{-i(\omega t-\Phi 2)} = X4$ = displacement of soil layer 2

Rewrite equations using above identities and expand.

Frame equation

$$-m_f\omega^2X1 = -k_fX1+k_fX2+d_fi\omega X1-d_fi\omega X2$$

Frame and drum equation

$$-m_f\omega^2X1-m_d\omega^2X2 = -k_{e1}X2+k_{e1}X3-k_{p1}X2+k_{p1}X3+i\omega d_1X2-i\omega d_1X3+F_e$$

Frame, drum, and layer 1 equation

$$-m_f\omega^2X1-m_d\omega^2X2-m_1\omega^2X3 = -k_{e2}X3+k_{e2}X4-k_{p2}X3+k_{p2}X4+i\omega d_2X3-i\omega d_2X4+F_e$$

Frame, drum, layer 1, and layer 2 equation

$$-m_f\omega^2X1-m_d\omega^2X2-m_1\omega^2X3-m_2\omega^2X4 = F_e$$

Set above equations equal to zero and collect terms (characteristics of the X's) to form the matrix of equations that describe the factors that effect the movement or displacement of each component:

Frame equation:

$X1(-m_f\omega^2+k_f-d_fi\omega)$
$X2(-k_f+d_fi\omega)$

Frame and drum equation:

$X1(-m_f\omega^2)$
$X2(-m_d\omega^2+k_{e1}+k_{p1}-i\omega d_1)$
$X3(-k_{e1}-k_{p1}-i\omega d_1)$

Frame, drum, and layer 1 equation:

$X1(-m_f\omega^2)$
$X2(-m_d\omega^2)$
$X3(-m_1\omega^2+ke2+k_{p2}-i\omega d_2)$
$X4(-ke2-k_{p2}-i\omega d_2)$

Frame, drum, layer 1, and layer 2 equation:

$X1(-m_f\omega^2)$
$X2(-m_d\omega^2)$
$X3(-m_1\omega^2)$
$X4(-m_2\omega^2)$

Collect terms:

$X1((-m_f\omega^2+k_f-d_fi\omega)+(-m_f\omega^2)+(-m_f\omega^2)+(-m_f\omega^2))= 0$

$X2((-k_f+d_fi\omega)+(-m_d\omega^2+k_{e1}+k_{p1}-i\omega d_1)+(-m_d\omega^2)+(-m_d\omega^2))=F_e$

$X3((-k_{e1}-k_{p1}-i\omega d_1)+(-m_1\omega^2+ke2+k_{p2}-i\omega d_2)+(-m_1\omega^2))=F_e$

$X4((-ke_2-k_{p2}-i\omega d_2)+(-m_2\omega^2))=F_e$

The above equations can be grouped together to form a 4 x 4 matrix with the X vectors representing the unknowns and the other terms on the left hand side of the equations representing characteristics. The terms on the right hand side of the equation are the knowns.

To simplify the housekeeping of the matrix manipulation, write the matrix as follows:

$$\begin{vmatrix} A11 & A12 & A13 & A14 \\ A21 & A22 & A23 & A24 \\ A31 & A32 & A33 & A34 \\ A41 & A42 & A43 & A44 \end{vmatrix} * \begin{vmatrix} X1 \\ X2 \\ X3 \\ X4 \end{vmatrix} = \begin{vmatrix} 0 \\ F_e \\ F_e \\ F_e \end{vmatrix}$$

Where,

$A11=(-m_f\omega^2+k_f-d_fi\omega)$

$A12=(-k_f+d_fi\omega)$

$A13=0$

$A14=0$

$A21=(-m_f\omega^2)$

$A22=(-m_d\omega^2+k_{e1}+k_{p1}-i\omega d_1)$

$A23=(-k_{e1}-k_{p1}-i\omega d_1)$

$A24=0$

$A31=(-m_f\omega^2)$

$A32=(-m_d\omega^2)$

$A33=(-m_1\omega^2+ke2+k_{p2}-i\omega d_2)$

$A34=(-ke2-k_{p2}-i\omega d_2)$

$A41=(-m_f\omega^2)$

$A42=(-m_d\omega^2)$

$A43=(-m_1\omega^2)$

$A44=(-m_2\omega^2)$

The determinant of a 4 x 4 matrix can be found by breaking the matrix into four 3 x 3 matrixes, multiplying the determinant of each 3 x 3 matrix by the appropriate characteristic from the first row of the matrix, and then summing the results. Because the last two terms (A13 and A14) in the first row of our 4 x 4 matrix are equal to zero, the contributing value of the determinants of the two 3 x 3 matrixes associated with the zero terms is zero.

$$\begin{vmatrix} A1 & A2 & A3 \\ B1 & B2 & B3 \\ C1 & C2 & C3 \end{vmatrix}$$

The determinant of the above 3 x 3 matrix is equal to:

A1B2C3-A1B3C2+A2B3C1-A2B1C3+A3B1C2-A3B2C1

Therefore, because A24 is equal to zero, the determinant of our 4 x 4 matrix is equal to:

A11((A22A33A44)-(A22A34A43)+(A23A34A42)-(A23A32A44))
-A12((A21A33A44)-(A21A34A43)-(A23A34A41)-(A23A31A44))

The values of the unknown terms (X1 through X4) can be found by taking the discriminant found by systematically substituting the unknowns into each column and dividing the result by the determinant of the original 4 x 4 matrix.

$$\begin{vmatrix} A11 & A12 & A13 & A14 \\ A21 & A22 & A23 & A24 \\ A31 & A32 & A33 & A34 \\ A41 & A42 & A43 & A44 \end{vmatrix}$$

Where,

A11= 0

A12=$(-k_f+d_fi\omega)$

A13=0

A14=0

A21=F_e

A22=$(-m_d\omega^2+k_{e1}+k_{p1}-i\omega d_1)$

A23=$(-k_{e1}-k_{p1}-i\omega d_1)$

A24=0

A31=F_e

A32=$(-m_d\omega^2)$

A33=$(-m_1\omega^2+ke2+k_{p2}-i\omega d_2)$

$A34=(-ke2-k_{p2}-i\omega d_2)$

$A41=F_e$

$A42=(-m_d\omega^2)$

$A43=(-m_1\omega^2)$

$A44=(-m_2\omega^2)$

The discriminant of the A11 column is:

$-F_eA12((A33A44)-(A34A43)+(A23A34)-(A23A44))$

By similar manipulation, the three remaining discriminants are as follows:

A12 column:

$F_eA11((A33A44)-(A34A43)+(A23A34)-(A23A44))$

A13 column:

$F_eA11((A22A44)-(A22A34)+(A34A42)-(A32A44))$
$-F_eA12((A21A44)-(A21A34)+(A34A41)-(A31A44))$

A14 column:

$F_eA11((A22A33)-(A22A43)+(A23A42)-(A23A32)+(A32A43)-(A33A42))$
$-F_eA12((A21A33)-(A21A43)+(A23A41)-(A23A31)+(A31A43)-(A33A41))$

Therefore, the displacements of each of the four model components can be calculated by the following four equations.

$$X1 = -F_e A12((A33A44)-(A34A43)+(A23A34)-(A23A44)) \div A11((A22A33A44)-(A22A34A43)+(A23A34A42)-(A23A32A44)) -A12((A21A33A44)-(A21A34A43)-(A23A34A41)-(A23A31A44))$$

$$X2 = F_e A11((A33A44)-(A34A43)+(A23A34)-(A23A44)) \div A11((A22A33A44)-(A22A34A43)+(A23A34A42)-(A23A32A44)) -A12((A21A33A44)-(A21A34A43)-(A23A34A41)-(A23A31A44))$$

$$X3 = F_e A11((A22A44)-(A22A34)+(A34A42)-(A32A44)) -F_e A12((A21A44)-(A21A34)+(A34A41)-(A31A44)) \div A11((A22A33A44)-(A22A34A43)+(A23A34A42)-(A23A32A44)) -A12((A21A33A44)-(A21A34A43)-(A23A34A41)-(A23A31A44))$$

$$X4 = F_e A11((A22A33)-(A22A43)+(A23A42)-(A23A32)+(A32A43)-(A33A42)) -F_e A12((A21A33)-(A21A43)+(A23A41)-(A23A31)+(A31A43)-(A33A41)) \div A11((A22A33A44)-(A22A34A43)+(A23A34A42)-(A23A32A44)) -A12((A21A33A44)-(A21A34A43)-(A23A34A41)-(A23A31A44))$$

Where,

$A11=(-m_f\omega^2+k_f-d_f i\omega)$

$A12=(-k_f+d_f i\omega)$

$A13=0$

$A14=0$

$A21=(-m_f\omega^2)$

$A22=(-m_d\omega^2+k_{e1}+k_{p1}-i\omega d_1)$

$A23=(-k_{e1}-k_{p1}-i\omega d_1)$

$A24=0$

$A31=(-m_f\omega^2)$

$A32=(-m_d\omega^2)$

$A33=(-m_1\omega^2+ke2+k_{p2}-i\omega d_2)$

$A34=(-ke2-k_{p2}-i\omega d_2)$

$A41=(-m_f\omega^2)$

$A42=(-m_d\omega^2)$

$A43=(-m_1\omega^2)$

$A44=(-m_2\omega^2)$

Development of the Excel Spreadsheet

Only the displacement of the roller drum was measured during the course of the field investigation of the RAM system. This meant that only the X2 equation could be used to test the model.

The X terms were identities that were used to simplify the development of the equation. They represented the displacement of each of the four model components which varied with time as a result of the variation in applied energy caused by the rotating eccentric mass. The measured roller drum deflections were based on the peak-to-peak accelerations. This meant that the maximum deflections were measured and that the effects of time and the lag angle were captured in the measured value of roller drum deflection.

VITA

Daniel Joseph Rich graduated from Rose-Hulman Institute of Technology in Terre Haute, Indiana with a B.S. in civil engineering in May 1992. He worked as a highway engineer for the Indiana Department of Transportation until he was called to active duty as an Air Force Civil Engineering officer in January 1993. His duty stations included Plattsburgh Air Force Base, Plattsburgh, New York; Riyadh Air Base, Riyadh, Saudi Arabia; and Osan Air Base, Osan, Republic of South Korea.

While in Korea, Dan earned his first professional engineering license from the State of Oregon in July 1996. He separated from the Air Force in January 1997 as a first lieutenant and moved to Houston, Texas. His military decorations include the Air Force Commendation Medal and the Air Force Achievement Medal, both with one oak leaf cluster, the Southwest Asia Service Medal with one device, and the National Defense Service Medal.

Dan's civilian careers have included facility engineer, forensic engineer, geotechnical engineer, and adjunct assistant professor. He earned his Master of Civil Engineering degree from the University of Houston in December 2001 and began his pursuit of a Doctor of Philosophy degree in Civil Engineering at Texas A&M University in September 2004. Dan was awarded his Ph.D. in December 2010. He founded Rich Engineering, a forensic civil engineering consulting firm, in June 2002 and continues to serve as the company's President and Chief Engineer. Dan became an Adjunct Assistant Professor within the Civil and Environmental Engineering Department at Prairie View A&M University in September 2008. He has taught introductory civil engineering design courses and upper level courses in geotechnical engineering, natural resources, materials testing and systems engineering.

Dan may be reached through Rich Engineering at 4950 FM 1960 West, Suite #A7, Houston, Texas 77069. His email address is danjrich@yahoo.com.